



Trigo-Rodríguez, J. M., Rimola, A., Tanbakouei, S., Cabedo Soto, V. and Lee, M. (2019) Accretion of water in carbonaceous chondrites: current evidence and implications for the delivery of water to early earth. *Space Science Reviews*, 215, 18. (doi:[10.1007/s11214-019-0583-0](https://doi.org/10.1007/s11214-019-0583-0))

There may be differences between this version and the published version. You are advised to consult the publisher's version if you wish to cite from it.

<http://eprints.gla.ac.uk/178376/>

Deposited on 28 January 2019

Enlighten – Research publications by members of the University of  
Glasgow

<http://eprints.gla.ac.uk>

1                   **ACCRETION OF WATER IN CARBONACEOUS**  
2                   **CHONDRITES: CURRENT EVIDENCE AND IMPLICATIONS**  
3                   **FOR THE DELIVERY OF WATER TO EARLY EARTH**

4  
5                   **Josep M. Trigo-Rodríguez<sup>1,2</sup>, Albert Rimola<sup>3</sup>, Safoura Tanbakouei<sup>1,3</sup>, Victoria Cabedo**  
6                   **Soto<sup>1,3</sup>, and Martin Lee<sup>4</sup>**

7  
8                   <sup>1</sup> Institute of Space Sciences (CSIC), Campus UAB, Facultat de Ciències,  
9                   Torre C5-parell-2<sup>a</sup>, 08193 Bellaterra, Barcelona, Catalonia, Spain. E-mail: trigo@ieec.uab.es

10                   <sup>2</sup> Institut d'Estudis Espacials de Catalunya (IEEC), Edif. Nexus,  
11                   c/Gran Capità, 2-4, 08034 Barcelona, Catalonia, Spain

12                   <sup>3</sup> Departament de Química, Universitat Autònoma de Barcelona, 08193 Bellaterra, Catalonia, Spain.  
13                   E-mail: albert.rimola@uab.cat

14                   <sup>4</sup> School of Geographical and Earth Sciences, University of Glasgow, Gregory Building, Lilybank  
15                   Gardens, Glasgow G12 8QQ, UK.

16  
17                   Manuscript Pages: 10

18                   Tables: 2

19                   Figures: 10

20  
21                   **Keywords:** comet; asteroid; meteoroid; meteorite; minor bodies; primitive; tensile strength  
22                   Accepted in Space Science Reviews (SPAC-D-18-00036R3, *Vol. Ices in the Solar System*)

23  
24                   **Abstract:**

25                   Protoplanetary disks are dust-rich structures around young stars. The crystalline and  
26                   amorphous materials contained within these disks are variably thermally processed and  
27                   accreted to make bodies of a wide range of sizes and compositions, depending on the  
28                   heliocentric distance of formation. The chondritic meteorites are fragments of relatively small  
29                   and undifferentiated bodies, and the minerals that they contain carry chemical signatures  
30                   providing information about the early environment available for planetesimal formation. A  
31                   current hot topic of debate is the delivery of volatiles to terrestrial planets, understanding that  
32                   they were built from planetesimals formed under far more reducing conditions than the  
33                   primordial carbonaceous chondritic bodies. In this review, we describe significant evidence for  
34                   the accretion of ices and hydrated minerals in the outer protoplanetary disk. In that distant  
35                   region highly porous and fragile carbon and water-rich transitional asteroids formed, being the  
36                   parent bodies of the carbonaceous chondrites (CCs). CCs are undifferentiated meteorites that  
37                   never melted but experienced other physical processes including thermal and aqueous  
38                   alteration. Recent evidence indicates that few of them have escaped significant alteration,  
39                   retaining unique features that can be interpreted as evidence of wet accretion. Some examples  
40                   of carbonaceous chondrite parent body aqueous alteration will be presented. Finally, atomistic  
41                   interpretations of the first steps leading to water-mediated alteration during the accretion of  
42                   CCs are provided and discussed. From these new insights into the water retained in CCs we  
43                   can decipher the pathways of delivery of volatiles to the terrestrial planets.

## 44 1. Introduction

45

46 Protoplanetary disks are dust-rich structures around young stars. They are flattened clouds of  
47 billions of particles whose compositions vary in response to environmental gradients created  
48 by intense electromagnetic and particle irradiation from the young star (see e.g., Martínez-  
49 Jiménez et al., 2017). There is growing evidence that stars like the Sun are often formed in  
50 stellar associations or even clusters (Trigo-Rodríguez et al., 2009). The dust-rich environments  
51 surrounding young stars have been observed, and reviewed extensively (see e.g., Armitage,  
52 2011) but information about the accretionary processes at work in the outer regions of these  
53 disks, where they pass into interstellar space, are still lacking. It is in such regions that the  
54 parent bodies of the carbonaceous chondrite meteorites (CCs) are believed to have formed  
55 (Weisberg et al., 2006). The lead-lead isotopic chronometer indicates that these rocks  
56 consolidated about 4.56 Ga ago from mineral condensates formed from the vapor phase at least  
57 since 4.567 Ga (Amelin et al., 2002). A current hot topic of debate is the delivery of water to  
58 terrestrial planets that were formed under far more reducing conditions than carbonaceous  
59 chondritic bodies (Alexander et al., 2018)

60

61 Disk instabilities, probably induced by the formation of giant planetary embryos, contributed  
62 to creating turbulence and size-sorting of disk materials (Boss, 2013). This process has been  
63 observed as noticeable dust clustering forming distinguishable rings in protoplanetary disks;  
64 e.g., the disk recently observed in HL Tau by the Atacama Large Millimeter/submillimeter  
65 Array (ALMA) (Zhang et al., 2015). The objects formed are no larger than few tens of  
66 kilometers so that the heat released from their radioactive components is quickly irradiated to  
67 space. These bodies have escaped chemical segregation (i.e., are undifferentiated) and so retain  
68 primordial disk components.

69

70 Meteorite evidence suggests that planetesimals became kilometer-sized bodies in the inner disk  
71 within about 10 millions of years from the formation of Ca- and Al-rich inclusions (CAIs).  
72 These planetesimals accreted to make planetary embryos, from which the terrestrial planets  
73 formed over timescales of few tens of millions of years. This epoch was marked by huge  
74 impacts that compacted and sculpted asteroids, transforming many such objects into collisional  
75 shocked, brecciated, and complex rubble piles (Trigo-Rodríguez and Blum, 2009). Such  
76 processes, however, affected not all of them. Some asteroids stored in the outer regions of the  
77 disk were probably less highly collisionally processed, and are enriched in organic and volatile  
78 compounds, as revealed the study of the comets 81P/Wild 2 and 67/Churyumov-Gerasimenko  
79 (Brownlee et al., 2006; Schulz et al., 2015). Remarkably, laboratory simulations of materials  
80 accreting at similar relative velocities end with meteorite proxies that are highly porous and  
81 fluffier than current chondrites (see e.g., Blum et al., 2006).

82

83 As planetesimals were the building blocks of planets, it follows that their composition played  
84 a central role in determining the constituents of planetary bodies. An important point on the  
85 composition of planetesimals is the initial rock/ice ratio because if enough volatiles were  
86 efficiently incorporated in the planetesimals, it implies a very different evolutionary track.

87 Once accretion was completed, it was thought that the radioactive components (mostly  $^{26}\text{Al}$   
88 and  $^{60}\text{Fe}$ ) produced enough internal heating to melt ices. The aqueous fluids generated  
89 interacted with primary phases to form the secondary minerals found in chondrites. Where  
90 insufficient radioactive heat was available, as found by Kunihiro et al. (2004), other processes  
91 such as shock compaction probably released water locally and over relatively short timescales  
92 (Trigo-Rodríguez et al., 2006; Trigo-Rodríguez and Blum, 2010; Rubin, 2012; Lindgren et al.,  
93 2015). The interaction of water with minerals typically involves elemental mobilization  
94 through dissolution, and precipitation of reaction products. This process is of paramount  
95 importance in some undifferentiated meteorites such as carbonaceous and ordinary chondrites  
96 (Jewitt et al., 2007).

97

98 The name chondrite originates from the rounded silicate spherules called chondrules, which  
99 together with CAIs are the main constituents of most chondrite classes apart for the most highly  
100 aqueously altered ones (i.e., some CM and all CI chondrites). Chondrules consist of refractory  
101 silicate minerals and opaque phases (e.g., metal and sulphide), and are dominant components  
102 of these meteorites that come from parent bodies that experienced hydrothermal activity (Dyl  
103 et al., 2012), with the exception again of CI chondrites (Brearley and Jones, 1998). These  
104 macroscopic components are enclosed by a fine-grained matrix containing micrometric or even  
105 nanometric particles, some of which originated in other stars; i.e., the so-called presolar grains.  
106 The porous nature of such fine-grained aggregates makes them potential places to preserve and  
107 retain ices and hydrated phases that were present in the outer disk (Abreu and Brearley, 2010;  
108 Moyano-Camero et al., 2016; Stroud et al., 2016; Singerling and Brearley, 2017). There is  
109 evidence in the literature of the action of water in some of these components of chondrites, an  
110 aspect on which this review is focused.

111

112 Consequently, the chondrites are conglomerates of fine dust (a mixture of silicates, oxides,  
113 metal, sulphides and organic constituents), chondrules and CAIs of different sizes and  
114 proportions (Brearley & Jones, 1998). It was proposed that the chondrites came from  
115 undifferentiated bodies because the materials from which they formed are heterogeneous in  
116 chemical and isotopic composition. However, new paleomagnetic results are challenging this  
117 probably simplistic scenario with presumably larger parent bodies (Carporzen et al., 2011;  
118 Shah et al., 2017). In fact, many CI and CM chondrites have being metamorphosed to some  
119 extent (Rubin et al., 2007) and they could have experienced thermal annealing linked to post-  
120 impact shock (Rubin, 2004).

121

122 The chondrites comprise carbonaceous, ordinary, enstatite, Rumuruti (R) and anomalous  
123 (ungrouped) classes, which in turn are subdivided into 15 groups (Weisberg et al., 2006). Each  
124 group displays different degrees of thermal or aqueous alteration (see the reviews by Brearley  
125 & Jones, 1998; Dobrică and Brearley, 2014), with some of the thermal processing potentially  
126 taking place by solar heating at short perihelion distances (Marchi et al., 2009; Trigo-Rodríguez  
127 et al., 2009). Remarkably, all chondrites are described as chemically primitive because the  
128 ratios of their major, non-volatile elements (Fe, Si, Mg, Al, Ca, etc...) are close to those  
129 observed in the Sun (Anders and Grevese, 1989; Lodders, 2003). In particular, CI, CM, and

130 CR groups are those that experienced a higher degree of parent body aqueous alteration (Rubin  
131 et al., 2007; Abreu and Brearley, 2010; Trigo-Rodríguez et al., 2015). The CR group is  
132 recognized as being especially pristine and can record early solar system processes in between  
133 the fine-grained textures of their matrices (Abreu and Brearley, 2010; Moyano-Camero et al.,  
134 2016). Many chondrite groups contain secondary minerals that indicate they experienced  
135 thermal metamorphism and aqueous processing (Table 1).

136

137 This review aims to provide additional insights into the presence of accretionary ice and  
138 hydrated phases in carbonaceous asteroids by describing and interpreting the evidence  
139 available in CM and CR carbonaceous chondrites. Our interpretations are compared with recent  
140 models and results in the scientific literature.

141

## 142 **2. Instrumental procedures.**

143

144 We have analyzed several carbonaceous chondrites with clear evidence for the action  
145 of water (Table 1). Our technical procedure is conventional with 20 µm thin sections of each  
146 meteorite studied microscopically using the following techniques. Mineral compositions were  
147 determined when further understanding of the effects of aqueous alteration in each meteorite  
148 was required.

149

150 Table 1

151

### 152 2.1. Petrographic Microscope

153

154 At the clean meteorite laboratory of the Institute of Space Sciences we use a Zeiss  
155 Scope, with magnifications up to 500X, and with a Motic BA310Pol Binocular microscope.  
156 This technique was used to study properties such as undulatory extinction, mosaicism,  
157 pleochroism, interference colours (with crossed nicols), mineral microstructures, etc. It is an  
158 interesting way for starting to recognize principal features and minerals and enables a great  
159 deal of information if used accurately. With this instrument we can distinguish the action of  
160 water in some minerals as shown by the presence of aqueously formed minerals, for example  
161 phyllosilicates. Crystalline silicate phases become diffuse and with distinguishable alteration  
162 colors when transformed into serpentine or other phyllosilicates. In addition, we also sought  
163 evidence for lineations and fractures as they denote the existence of preferential shock  
164 compaction.

165

### 166 2.2. Scanning Electron Microscopy (SEM)

167

168 Samples were studied at the *Institut Català de Nanociència i Nanotecnologia* (ICN2)  
169 using a FEI Quanta 650 FEG with a Back Scattered Electron Detector (BSED). The Quanta  
170 650 was operated in low-vacuum mode with each thin section uncoated, and EDS analyses  
171 were used to obtain X-Ray spectra and semi-quantitative composition from specific points.  
172 Secondary Electron (SE) and Back-Scattered Electron (BSE) imaging was used to study in

173 detail sites of interest in the sample, with magnifications up to 30,000 X. The SEM was also  
174 used to select regions of interest (ROIs) for subsequent chemical analysis by electron  
175 microprobe and EDS.

176

### 177 2.3. Energy-Dispersive X-ray Spectroscopy (EDS)

178

179 We characterized the mineralogy of the thin sections by performing non-destructive  
180 EDS analysis by SEM. EDS was used to create elemental maps of the ROIs (Fig. 3). The EDS  
181 detector was an Inca 250 SSD XMax20 with Peltier cooling and with a detector area of 20  
182 mm<sup>2</sup>, attached to the SEM at the Institut Català de Nanociència i Nanotecnologia (ICN2).

183

### 184 2.4. Electron microprobe

185

186 BSE imaging and electron microprobe analyses were performed using a JEOL JXA-  
187 8900 electron microprobe equipped with five wavelength-dispersive spectrometers at the  
188 Universitat de Barcelona. The electron microprobe fires an electron beam at the sample, and  
189 detects the characteristic X-rays emitted by each element, when electrons from higher energy  
190 shells fill the vacancies left by the electrons scattered by the beam. The energy of the X-rays is  
191 characteristic of the difference in energy between two electron shells, and of the atomic  
192 structure of the element, which enables quantitative elemental analysis of the specimen.

193

### 194 2.5. Ultra High Resolution Transmission Electron Microscopy (UHRTEM).

195

196 In order to study the mineral structure of CM chondrites at the nanoscale, chips of two  
197 meteorites (Murchison and Cold Bokkeveld) that were ion thinned to electron transparency  
198 using a Fischione 1050 model Ar ion mill at CIC (Granada University). The samples were  
199 then studied using a FEI Titan G2 60-300 microscope at CIC with a high brightness electron  
200 gun (X-FEG) operated at 300 kV and equipped with a Cs image corrector (CEOS). Analytical  
201 electron microscopy (AEM) used a SUPER-X silicon-drift windowless EDX detector. The X-  
202 ray spectra were collected in STEM (Scanning Transmission Electron Microscopy) mode with  
203 imaging using a HAADF (High Angle Annular Dark Field) detector. Digital X-Ray maps were  
204 also collected on selected areas of the samples. For quantitative analyses the EDX data were  
205 corrected using the thin-film method (Cliff and Lorimer, 1975; Lorimer and Cliff, 1976) with  
206 K-factors determined using mineral standards: albite (Na, Al), anorthite (Al, Ca),  
207 anorthoclase (Na, Al), Augite (Mg, Al, Ca & Fe), biotite (Mg, Al, K, Fe), scapolite (Na, Al,  
208 Ca), spessartine (Al, Mn), hemimorphite (Zn), microcline (Al, K), muscovite (Al, K), olivine  
209 (Mg, Fe), rhodonite (Mn, Fe), titanite (Ca, Ti), and osumilite (Mg, Al, K, Fe). The resulting  
210 KAB factors were: Na 1.18 (0.03), Mg 1.10 (0.03), Al 1.00 (0.02), Si 1.00, K 1.12 (0.04), Ca  
211 1.03 (0.03), Ti 1.28 (0.04), Mn 1.33 (0.01), Fe 1.37 (0.03) and Zn 1.53 (0.01). Atomic  
212 concentration ratios were converted into formulae according to stoichiometry (number of O  
213 atoms in theoretical formulae).

214

215

### 3. Results: Evidence of accretionary phases in CM and CR chondrites

This section focuses on describing evidence in CCs for accretion of hydrated phases. The best evidence is found in some CM and CR chondrites for which water availability was limited. Once the hydrated minerals had been incorporated into these meteorites, the water could have been released by moderate heating from three main sources: self-gravity, collisional compaction, and radiogenic decay. It is worth mentioning that self-gravity is an unlikely heat source because the CM chondrites probably had a parent body of few tens of km of diameter, but this process cannot be discounted completely.

As a consequence of aqueous alteration, minor phases grew in the pores of these chondrites. The alteration products in Murchison and other CM chondrites have been widely described in previous papers (e.g., Fuchs et al., 1973; Trigo-Rodríguez et al., 2006; Rubin et al., 2007). Here we focus on two CMs, namely Murchison and MET 01070, and two CR chondrites, namely Renazzo, and GRA 95229.

#### 3.1. CM CHONDRITE GROUP

CM chondrites are breccias and aqueously altered rocks that contain up to ~9 wt. % indigenous water, mostly bound in phyllosilicates (Bischoff et al., 2006; Rubin et al., 2007). All CM chondrites have undergone extensive parent body aqueous alteration, and the products of these reactions obscure evidence for primordial accretionary processes. The porous matrices of most CM chondrites contain clumps of minerals formed by aqueous alteration, consisting mainly of phyllosilicate and tochilinite intergrown with pentlandite and Ni-bearing pyrrhotite. A full description of these phases is in Rubin et al. (2007).

Parent body heating was originally proposed to have been mild in the CM and CR groups, as the maximum inferred temperatures in both CC groups are 50 °C and <150 °C, respectively (Zolensky et al., 1993). Now we know that some of the CCs were thermally metamorphosed at temperatures of up to 800 °C and above after aqueous alteration (Garenne et al., 2014; Doyle et al., 2015; King et al., 2017). Aqueous alteration produces changes in the silicates that are transformed into phyllosilicates (Velbel and Palmer, 2011, Velbel et al., 2012). This suggests that collisions also affected the bulk chemistry of their parent bodies, and probably participating to some extent in aqueous alteration and compaction of the different groups (Zolensky and McSween, 1988; Zolensky et al., 2008). An extended chronology for the setting of aqueous alteration has been given by Lee et al. (2012).

A new aqueous alteration sequence for CM chondrites has been proposed that provides evidence of progressive aqueous alteration, ranging from type 3.0 (pristine, unaltered materials) to type 2.0 (highly altered rocks, formerly classified CM1) (Rubin et al., 2007). Some alteration features in CMs result from processes that went to completion at the beginning of the alteration sequence, such as alteration of primary igneous glass in chondrules, production of aqueous altered minerals, and the formation of secondary sulphide grains. Other petrologic

259 properties reflect processes active throughout the alteration sequence: formation of  
260 phyllosilicates, oxidation of metallic Fe-Ni, destruction of isolated matrix silicate grains,  
261 alteration of chondrule phenocrysts, changes in the composition of secondary minerals, and the  
262 precipitation of carbonates (Trigo-Rodríguez et al., 2006). Most CM chondrites have  
263 experienced different degrees of aqueous alteration, but some chemically linked ungrouped  
264 chondrite like e.g. Acfer 094 seems to have largely escaped it and have remained pristine  
265 (Rubin et al., 2007).

266

### 267 3.1.1. MURCHISON CHONDRITE

268

269 Murchison is one of the least aqueously altered CM chondrites, in common with  
270 Murray, but the extent of hydration of both meteorites is heterogeneous (Trigo-Rodríguez et  
271 al., 2006; Rubin et al., 2007; Trigo-Rodríguez et al., 2015). There is no doubt that the collisions  
272 had significant effects in the evolution of the parent body of CM chondrites (Trigo-Rodríguez  
273 et al., 2006; Rubin, 2012). The petrographic texture is complex, and Murchison is a breccia  
274 (Rubin et al., 2007). Murchison has type-I chondrules with tochilinite inclusions, metal grains  
275 and it has many spherical troilite and pyrrhotite grains in its matrix. Tochilinite appears as a  
276 single phase but it exhibits variable composition, and is correlated with P-bearing sulfides,  
277 which are associated with pyroxene and forsterite (Palmer and Lauretta, 2011). Even though  
278 tochilinite and P-bearing sulfides are the common phases, tochilinite also contains chromium-  
279 rich phases

280

281 Metal grains in Murchison often have aureoles that are composed mainly of oxides and  
282 formed by corrosion (Hanowski and Brearley, 2000). Aqueous alteration minerals also occur  
283 in the fine-grained matrix and include sulphides and carbonates that precipitated from water  
284 (Trigo-Rodríguez et al., 2006; Rubin et al., 2007; Lee et al., 2014). It seems likely that most  
285 chondrules accreted into the parent body with a fine-grained porous mantle that probably  
286 hosted hydrated minerals or even dirty ices (Figure 1). The secondary minerals preferentially  
287 grew where the pores were available within chondrule mantles and the surrounding matrix, and  
288 the variable sizes of crystals and textures probably reflects the presence of volatile phases that  
289 disappeared under the action of moderate heat and aqueous processing, probably associated  
290 with shock compaction (Trigo-Rodríguez and Blum, 2010). Radiogenic heating and collisional  
291 compaction are processes that probably produced moderate heat that helped evaporation of the  
292 volatiles, but leaving aqueous alteration minerals when the components in solution precipitated  
293 into the pores of the meteorite. The way in which the aqueous alteration proceeded from highly  
294 porous progenitors retaining volatiles in their interior has been described in detail (Trigo-  
295 Rodríguez et al., 2006; Rubin et al., 2007).

296

297 Figure 1

298

299 Aqueous alteration of Murchison chondrules is not pervasive, with some areas being  
300 more highly altered than others (Lee and Lindgren, 2016). This is nicely shown in Figures 2  
301 and 3. Figure 2 is a backscattered electron (BSE) image of a chondrule whose rim is diffuse,



302 apart for on the left hand side (square inset region, Fig. 2a,c). Fig. 2c,d illustrates a corroded  
303 metal grain contained in the chondrule. It is also possible to follow a line of Fe-oxides that  
304 penetrates into the chondrules, which can be seen particularly well in Fig. 3a. Some S and Ca  
305 are also associated with such aqueous alteration minerals produced in the interior of the  
306 chondrules (sulphides and carbonates are common as well).

307

308           Figures 2, and 3

309

310           Our previous nanoscale study of Murchison identified a chemically unequilibrated  
311 matrix that is highly heterogeneous under HRTEM examination (Trigo-Rodríguez et al., 2017).  
312 Micrometer-sized windows of Murchison matrix display characteristic layering of  
313 phyllosilicates associated with highly reactive metal grains and sulphides. These minerals  
314 exemplify an extraordinary accretionary diversity in this meteorite and highlight the need to  
315 study other highly unequilibrated chondrites to confirm the existence of hydrous mineral  
316 phases in the protoplanetary disk (see e.g. Fegley and Prinn, 1989; Lodders and Fegley, 2011).  
317 We think that this nanoscale complexity may be indicative of the formation conditions of this  
318 meteorite, and the minimal thermal processing that occurred in its parent asteroid.

319 We have additionally investigated CM2 chondrites to seek evidence for the incorporation of  
320 hydrated phases and ices into the parent body, which may be best identified using nanoscale  
321 observations b UHRTEM (Trigo-Rodríguez et al., 2017). To highlight the level of aqueous  
322 alteration of the matrix we include here an image of Murchison matrix obtained using the  
323 technique. The defined areas in Figure 4 correspond to: 1) Troilite (FeS), 2) Talc, 3-8) Mg-rich  
324 serpentine, 9) calcic amphibole, and 10) calcic pyroxene. The bright spots in the Fe+S images  
325 are clearly troilite that are adjacent to phyllosilicates that have suffered significant parent body  
326 alteration. In fact, Brearley (1997) described that clinoenstatite have been altered to amphibole  
327 and talc (two of the identified minerals in our ROIs #2 and #9) nearby contraction cracks in the  
328 case of CV3 carbonaceous chondrite Allende. It is well known that parent body aqueous  
329 alteration usually leads to a progressive loss of Mg-rich anhydrous silicates because the Mg  
330 goes into the fluid and precipitates to form Mg-rich phyllosilicates (Trigo-Rodríguez et al.,  
331 2006; Rubin et al., 2007).

332

333           Probably due to extensive parent body aqueous alteration no clear evidence for pre-  
334 accretionary hydrated phases in carbonaceous chondrites has been published. Our working  
335 hypothesis is that extensive aqueous alteration often predates the oldest evidence of  
336 accretionary hydrated minerals. The CM2 chondrite Murchison is particularly interesting  
337 because it is a breccia that contains regions with different degrees of aqueous alteration,  
338 probably due to limited water availability. In this sense, we found that some ROIs of Murchison  
339 have escaped extensive interaction with water (Rubin et al., 2007). Less altered regions contain  
340 highly reactive phases along with phyllosilicates, sulphides and oxides (see Fig. 4, and Trigo-  
341 Rodríguez et al., 2017). It is difficult to understand the co-existence of reactive minerals (like  
342 e.g. FeS) with hydrated phases at this fine scale. As a consequence, we envision that these  
343 minerals were probably stacked together in the aggregate structure, and scarcely affected by  
344 extensive parent body aqueous alteration. If we are correct, the relative absence of evidence for

345 accreted hydrated minerals could be direct consequence of the bias imposed when we study  
346 CCs at microscale. We should undertake more studies of pristine meteorites at the nanoscale  
347 given that theoretical predictions and observations of presolar grains and IDPs indicate that the  
348 minerals available in the protoplanetary disk were nanometric (Zinner, 2003; Lodders and  
349 Amari, 2005; Lodders and Fegley, 2011). We have noticed that the matrix of Cold Bokkeveld,  
350 the other CM2 studied using UHRTEM, is much more highly altered (Trigo-Rodríguez et al.,  
351 2017). In consequence, given the different degree of aqueous alteration found in CM chondrites  
352 (Rubin et al., 2007), only these experiencing moderate parent body alteration (like e.g.  
353 Murchison) could be of use in the search of pre-accretionary hydrated minerals.

354

355 In view of current evidence it is difficult to make any definitive statements about wet  
356 accretion, but we think this should not be ruled out without additional studies of the  
357 carbonaceous chondrites at nanometre scale. Probably using existing techniques to study these  
358 rocks at the nanoscale evidence of pre-accretionary hydrated minerals could be obtained. We  
359 hope that our interpretation of the matrix mineralogy of Murchison can promote further  
360 research into the possibility that carbonaceous chondrites contain nanoscale evidence of wet  
361 accretion.

362

363 Figure 4.

364

### 365 3.1.2. MET 01070 CM2 CHONDRITE

366

367 We have chosen the CM2.0 MET 01070 because it has suffered pervasive aqueous  
368 alteration, and exhibits long lenses probably caused by precipitation from an aqueous fluid (see  
369 Fig. 5 and Rubin et al., 2007). The lenses are formed of aqueous alteration products, range  
370 appreciably in thickness, and surround large chondrule pseudomorphs. We conclude that these  
371 lenses were produced when a water-rich front with various elements in solution precipitated  
372 phases containing Ca, P, Ni, and S. As consequence of this process, Ca-carbonate (mainly  
373 CaCO<sub>3</sub>) and Ca-phosphate grains were produced within the lens. In order to form this  
374 precipitation front, a substantial volume of water was needed within the parent body perhaps  
375 due to a thermal gradient or to compaction. Other phases within the lens are Ni-bearing sulfide  
376 (e.g. pentlandite), which are present in the meteorite matrix (Table 2).

377

378 Figure 5.

379

380 These kind of extended lenses are not usual in CMs, and are clearly a consequence of  
381 extensive aqueous alteration (Rubin et al., 2007). The significant aqueous alteration differences  
382 observed in specimens of the most pristine CM and CRs suggest that water availability was  
383 probably limited for most of them (see Trigo-Rodríguez, 2015 and references therein). These  
384 observations associated with pristine chondrites are of key relevance in the search for evidence  
385 of hydrated minerals or ices accreted from the protoplanetary disk. We predict that the accretion  
386 of such water-rich phases should produce distinctive aqueous alteration typically being local  
387 and nearly static in nature.

388

## 3.2. CR CHONDRITE GROUP

389

390

391

392

393

394

395

396

397

398

399

400

401

402

403

404

This group of chondrites is of key interest with regards to the evolution of volatile-rich species in the protoplanetary disk. The CR group has large chondrules, ranging from 0.8 to 4.4 mm in diameter, with an abundance of 40 to 60 vol % (Hutchison, 2004). These chondrules are rich in forsterite ( $\text{Mg}_2\text{SiO}_4$ ), enstatite ( $\text{MgSiO}_3$ ) and Fe,Ni-metal rich inclusions. They have conspicuous rims of metals and silicates, which could have been formed by processes taking place either within the protoplanetary disk or during accretion. The fine-grained matrix is dark and optically opaque and comprises up to 30-51 vol % of the meteorites. It is mainly composed of olivine, but also contains carbonates, pyrrhotite ( $\text{Fe}_{1-x}\text{S}$ ;  $x = 0$  to 0.2), which is a variant of troilite (FeS), pentlandite ( $(\text{Ni,Fe})_9\text{S}_8$ ), magnetite ( $\text{Fe}_3\text{O}_4$ ), serpentine ( $(\text{Mg,Fe})_3\text{Si}_2\text{O}_5(\text{OH})_4$ ) and chlorides (Brearley and Jones, 1998; Abreu and Brearley, 2010). CAIs are rare ( $<3$  vol %) but where present are rich in melilite ( $(\text{Ca,Na})_2(\text{Al,Mg,Fe}^{2+})$ ) and spinel ( $\text{MgAl}_2\text{O}_4$ ) and also contain silicates and other oxides. CR chondrites also contain dark phyllosilicate rich inclusions ( $<8$  vol %), Fe-Ni metal inclusions (5-8 vol %) and sulfides (1-4 vol %) (Trigo-Rodríguez, 2012).

405

406

407

408

409

410

411

412

413

414

415

416

417

418

The CRs contain minerals that have experienced much less parent body aqueous alteration than the CMs so that pre-accretionary processes **could be** more apparent. For this reason we have selected this chondrite group for our discussion related to hydration processes in the protoplanetary disk. In general, the CR chondrites are composed of chondrules, fine-grained matrix, and usually tiny CAIs and ameboid-olivine aggregates (AOAs). Type-I forsteritic chondrules rich in Fe-Ni metal grains compise about ~96% of the chondrule population, type-II chondrules constitute ~3 %, while other types are minor (Schrader et al., 2013). The matrices of CR chondrites consist of abundant submicron Fe-rich hydrated amorphous silicate grains, mixed with nanometer-sized phyllosilicates and organics (Le Guillou and Brearley, 2014; Le Guillou et al., 2015; Alexander et al., 2017). These widespread oxidized and hydrated amorphous silicates provide clues of the alteration conditions and  $\text{H}_2$  degassing of asteroids. In the following sub-sections some interesting CR specimens are described in the context of possible evidence of post-accretionary aqueous alteration.

419

### 3.2.1. RENAZZO

420

421

422

423

424

425

426

427

428

429

Renazzo is a pristine CR chondrite that has avoided extensive parent-body thermal metamorphism. As a consequence its metal grains have escaped recrystallization, and are not mixed as kamacite and taenite phases (Wasson and Rubin, 2010). It is a nice example of meteorite that has undergone minor aqueous alteration, clearly much less than has been experienced by most of the CM chondrites described in previous section. Moreover, this meteorite was recovered soon after its fall, so that it has not undergone terrestrial alteration. For these reasons Renazzo has clues to processes of post-accretionary aqueous alteration that could be associated with direct modification of minerals by water derived from accreted hydrated phases or ices. To find definitive evidence in that regard we need to study the fine-

430 grained matrix that probably retained water in these two forms, as documented for LAP 02342  
431 CR chondrite (Moyano-Cambero et al., 2016; Stroud et al., 2016)

432

433 Petrographic evidence in support of the aforementioned scenario is that Renazzo  
434 exhibits features characteristics of static aqueous alteration (see e.g. Trigo-Rodríguez et al.,  
435 2006). This type of alteration occurs when water is scarce, and is highlighted by Fig. 6.  
436 Chondrule metal grains in the left hand side of the image have clear evidence of partial  
437 corrosion, as well as some minerals present near the chondrule's contact with the matrix.  
438 Mobilization of Fe, S and Ni has formed some tiny precipitates in the surrounding matrix, near  
439 the chondrule itself.

440

441 Figure 6.

442

443 Such features have been described previously in other CR3 chondrites (Abreu and  
444 Brearley, 2010), and these authors emphasized the importance of this chondrite group for  
445 understanding the first phases of planetesimal accretion. The matrices of some CR chondrites  
446 often have significant FeO-enrichments in comparison to the less altered ones, again indicating  
447 that the alteration could have operated at local scale and for a limited time. These observations  
448 are consistent with static aqueous alteration in the parent asteroid, so it probably requires the  
449 incorporation of water ice in the matrix of CCs. Then, water availability assured its  
450 incorporation to the structure of the minerals through chemical bonds, preserving it of escaping.

451

### 452 3.2.2. GRAVES NUNATAKS 95229

453

454 This selected meteorite is an altered CR2, and quite remarkable for its extraordinary  
455 abundance of amino acids. Most CR chondrites are breccias\*, and all are petrological type 2.  
456 Chondrules in GRA 95229 are large (<2 mm), with an abundance of 50 to 60 vol %. They are  
457 mainly composed of Fe-poor olivine and pyroxene. Chondrule rims are rare, poorly defined  
458 and often discontinuous (Abreu and Brearley, 2008). They are rich in Fe sulfides and magnetite  
459 (Brearley and Jones, 1998). Surrounding matrix regions are rich in silicates, with magnetite,  
460 rare Fe-Ni sulfides and chondrule fragments. GRA 95229 contains a large proportion of organic  
461 materials, e.g. amino acids like glycine, alanine and isovaline, in comparison with other CR  
462 chondrites. They are also more abundant than in almost all other primitive chondrites, such as  
463 CM2s Murchison and Murray, which have one of the larger organic matter proportions of all  
464 chondrites (Martins et. al., 2007).

465

466 Extensive aqueous alteration is evident in other CR chondrites (Trigo-Rodríguez,  
467 2015). Water played a major role in mobilizing specific elements and altered several mineral  
468 phases to produce carbonates, oxides and sulphides. In some cases the action of water was  
469 pervasive, particularly with regards to metal and troilite grains, and participated in the complete  
470 replacement of mineral grains located in the matrix. Pyrrhotite was replaced during aqueous  
471 alteration of the CR2 chondrites Graves Nunataks (GRA) 95229 and Elephant Moraine (EET)  
472 92159. After such replacement the voids were filled by submicron-sized magnetite grains. In

473 some cases the replacement is incomplete and some pyrrhotite remains. Interestingly, such  
474 growth of magnetite is expected to occur from the precipitation of Fe from a low-temperature  
475 aqueous solutions (see e.g. Fig. 7). A similar action of water on pyrrhotite grains has been  
476 observed in the Kaidun meteorite (Zolensky & Ivanov, 2003; Trigo-Rodríguez *et al.*, 2013).

477  
478 Fig. 7

### 479 480 3.2.3. La Paz 02342

481  
482 The LAP 02342 CR chondrite highlights how the Antarctic collection continued to  
483 provide new specimens of extraordinary cosmochemical interest. LAP 02342 has probably  
484 experienced a lower degree of aqueous alteration than other CR chondrites, and we have  
485 identified some clear signatures of accretion of ices in different components (Moyano-Camero  
486 *et al.*, 2016; Stroud *et al.*, 2016; Nittler *et al.*, 2019). This meteorite contains an unusual ~100  
487  $\mu\text{m}$  diameter highly C-rich clast that is composed of a fine-grained mixture of isotopically  
488 anomalous organic matter,  $^{16}\text{O}$ -poor Na-sulfates, crystalline and amorphous silicate grains  
489 (including GEMS - Glass with Embedded Metal and Sulfide), sulfides, and abundant  
490 presolar grains. The Na-sulfates surrounding the micro-xenolith are isotopically similar to  
491 the rare cosmic symplectite, likely reflecting the isotopic composition of a primordial water  
492 reservoir that accreted as ice within the clast (Nittler *et al.*, 2019). This ultra-carbonaceous clast  
493 may represent a cometary building block that accreted into the matrix of the CR chondrite  
494 parent asteroid. These observations are also consistent with hydrogen and nitrogen isotopic  
495 anomalies in organic matter retained in the fine-grained matrices of CCs that were probably  
496 inherited from other unsampled bodies of cometary nature present in the protoplanetary disk at  
497 the time of formation of carbonaceous chondrites (Busemann *et al.*, 2006)

498  
499 These pristine CR chondrites can also provide new clues about protoplanetary disk  
500 chemistry. LAP 02342 hosts a chondrule with a primordial S-rich mantle (Figure 8) altering  
501 the surrounding matrix (see e.g. Moyano-Camero *et al.*, 2016). It has been recently found that  
502 S chemistry was significant in protoplanetary disks (Fuente *et al.*, 2016). It is important to note  
503 that if such chemistry existed, primordial ices could be enriched in this element because S-  
504 bearing molecules can be slightly polar:  $\text{S}_2\text{H}$ ,  $\text{H}_2\text{S}$ ,  $\text{H}_2\text{S}_2$ ,  $\text{SH}$ , etc. so it is likely that they could  
505 easily attach to ices, and be accreted into ice-rich chondrule rims. According to these  
506 observations, and other isotopic observations of the rim described in Nittler *et al.* (2019), we  
507 found that this S-rich mantle is evidence for ice accretion in the chondrule rim. We interpreted  
508 the accretional signatures because, once on the CR host matrix, the sublimation of the ice  
509 promoted the formation of the observed  $^{16}\text{O}$ -poor Na-sulfates (Nittler *et al.*, 2019).

510  
511  
512 **Figure 8**

513  
514  
515

## 4. Discussion

### 4.1 Using the extent of aqueous alteration to understand pre-accretionary hydration

Parent bodies of the samples described here are carbon-rich asteroids that are highly unequilibrated mixtures of different materials, some crystalline and created close to the Sun, others formed at greater heliocentric distances. Most of these bodies accreted in the outer protoplanetary disk in the presence of ices, organics and hydrated mixtures. The most primitive materials coming from these bodies are very different to terrestrial rocks because they are chemically highly unequilibrated (Brearley & Jones, 1998). The rock-forming materials building the so-called transitional asteroids are probably closer to the materials forming comets, thus invoking a continuum between asteroid and cometary materials (Briani et al., 2011; Trigo-Rodríguez, 2015). The NASA Stardust mission confirmed that comet 81P/Wild 2 is also composed of micrometre-size refractory mineral grains blown by the stellar wind to their formation regions (Brownlee et al., 2006). Laboratory experiments (Blum et al., 2006) suggest that the comets were highly porous, so that they probably retained volatiles and hydrated phases during the early stages of Solar System formation. The relative absence of hydrous phases in grains collected during the Stardust mission was probably a consequence of heating during the capture process, which led to vaporization of the most volatile phases (Trigo-Rodríguez et al., 2008).

Thermochemical modeling suggests that some minerals formed in the protoplanetary disk were hydrated, and probably water was incorporated as ice- and carbon-rich aggregates (Lodders, 2003; Ebel, 2006). Despite expectations, evidence for the accretion of hydrated phases and ices in the CM and CR chondrites has remained elusive owing to overprinting by thermal metamorphism and aqueous alteration (Bischoff, 1998). Once the parent bodies were formed as aggregates (Blum et al., 2006), these volatile phases were compacted during collisions, and sublimed or liquefied to saturate the rock. For that reason it is very important to identify pristine CCs, and recent studies on CR chondrites are promising (Abreu and Brearley, 2010; Trigo-Rodríguez et al., 2015; Moyano-Camero et al., 2016).

To gain insight on the amount of water incorporated into the parent bodies of carbonaceous chondrites, Howard et al. (2015) quantified the modal abundances of major mineral phases (with abundances >1 wt.%) using Position Sensitive Detector X-ray Diffraction (PSD-XRD). They concluded that the variability between CCs in their measured hydration indicates that either accretion of ices was heterogeneous, or fluid was widely mobilized. Obviously, most meteorite samples are biased samples because they come from bodies that experienced collisions sufficiently energetic to launch the ejecta into heliocentric orbits (Beitz et al., 2016). Despite this current bias, which should be mitigated by future sample-return missions, Howard et al. (2015) found using PSD-XRD that the initial mass fraction of H<sub>2</sub>O inside of their parent asteroids was <20 wt.%. This suggests a relatively small fraction of hydrated phases and/or ices were incorporated, probably as minor constituents of meteorite matrices (Trigo-Rodríguez, 2015). Recent H-isotope investigations evidence also suggest two

559 different sources of accreted water in the CM chondrites (Piani et al., 2018). Most secondary  
560 minerals in CCs show O-isotopic signatures that are consistent with accretion of a source of  
561 water in the inner Solar System that became  $^{16}\text{O}$ -rich, while water related with outer minor  
562 bodies has the  $^{16}\text{O}$ -poor signature (Marrocchi et al., 2018; Nittler et al., 2019). This fact has  
563 been explained because Jupiter acted as a barrier precluding significant inward transport of  
564 outer solar system materials, with the probable exception of cometary fragments produced by  
565 tidal disruption during close approaches to the giant planets. An example for such contribution  
566 could be the  $^{16}\text{O}$ -poor Na-rich sulfates in the border of the C-rich micro-xenolith discovered by  
567 Nittler et al. (2018).

568

569 The study of primordial fayalite grains can be very relevant to understand the complex  
570 accretion scenario as was exemplified in Marrocchi et al. (2018) where the origin of water in  
571 CCs was investigated in CV chondrites using O isotopes hosted in several minerals. They  
572 conclude that the process controlling the O-isotopic composition of CV chondrites was related  
573 to the isotopic equilibrium between  $^{16}\text{O}$ -rich anhydrous silicates and a  $^{17}\text{O}$  and  $^{18}\text{O}$ -rich fluid.

574

575 Other aqueous alteration minerals including calcite are common in the different  
576 chondrite groups (Table 1), but the action of water produced distinctive mineralogy, which  
577 depends on each chondrite group, temperature and differences in the availability of liquid  
578 water. Our results clearly show that these often tiny mineral grains preferentially grew in the  
579 matrix pores (Trigo-Rodríguez et al., 2006; Lee et al., 2012, 2014). Most of the aqueous  
580 alteration seems to be static, short-time events that produced distinctive features like the  
581 aureoles in Murchison that formed around native metal grains by oxidation (Hanowski and  
582 Brearley, 2000). Calcite and other complex carbonates are also useful in dating hydration  
583 processes as their  $^{53}\text{Mn}$ - $^{53}\text{Cr}$  ages precise formation ages for minerals in the CI and CM  
584 chondrites (for an update see e.g. Fujiya et al., 2013). Results indicate that hydration of the CI  
585 parent body occurred between 3 and 9 Ma after formation of the CAIs, themselves dated to  
586 4.567 Ga (Amelin et al., 2002). Lee et al. (2012) found that some CM chondrites, for example  
587 Queen Elizabeth Range (QUE) 93005, have shorter alteration periods starting about 4 Ma after  
588 the formation of the oldest solar system solids. A recent study of CM2 carbonaceous chondrite  
589 Lonewolf Nunataks (LON) 94101 reveals that it is possible to decipher the existence of  
590 multiple carbonate generations from intrinsic oxygen isotope differences (Lee et al., 2012;  
591 2013).

592

593 A formation scenario for the Murchison CM2 chondrite involves a transitional asteroid  
594 that probably accreted both anhydrous and hydrous materials. Radiogenic heating contributed  
595 at an early stage to releasing part of the water that altered some materials, but only locally  
596 because the water was inhomogeneously distributed. Later on, because of successive impacts  
597 of the parent asteroid with other bodies a brecciated structure was created, the porosity of the  
598 matrix decreased and all the materials were significantly compacted (Trigo-Rodríguez et al.,  
599 2006). Chondrules and inclusions were tough objects that by their nature resisted compaction.  
600 For this reason it was in matrix material where the collisions had their greatest effects. Over  
601 time Murchison's materials started to fragment and comminute. Some primordial mantles were

602 detached and some aqueous alteration could act locally as a consequence of water release if  
603 direct evaporation did not occur. Due to all this collisional gardening most of the known CM  
604 chondrites are *breccias* of materials with diverse alteration or metamorphic histories, but finally  
605 built by impact processes (Hanna et al., 2015). As a consequence of multiple impacts  
606 experienced by chondritic asteroids since their formation (see e.g. Beitz et al., 2016), pore  
607 spaces collapsed and the materials were sheared, heated and shattered. Evidence for this  
608 scenario is the discovery of free mantles in the matrices of CM chondrites (Trigo-Rodríguez et  
609 al. 2006) that, even when probably they were accretionary in origin, also experienced  
610 compaction during shock events (Bland et al., 2014). These impacts could have promoted the  
611 release of liquid water, initiating aqueous alteration of some minerals and a mobilization of  
612 some elements that gave room for growth of secondary (or altered) minerals like these fine-  
613 grained aqueous alteration phases. To describe and date these processes is extremely important  
614 in an astrobiological perspective because aqueous alteration processes could have directly  
615 contributed to catalyse the extremely diverse organic species found in carbonaceous chondrites  
616 (Rotelli et al., 2016)

617

618 On the other hand, radiogenic heating of chondritic parent bodies was size-dependent  
619 and constrained during the first 10 Ma after their formation. We know this from the carbonates,  
620 whose mean size varies with the extent of aqueous alteration. The highly altered Alais and  
621 Tonsk CI meteorites have large carbonate grains (Endreß & Bischoff, 1996). This process is  
622 probably associated with the precipitation of minerals including carbonates, sulphides and  
623 phosphides in the matrices of these meteorites. These bodies accreted live  $^{53}\text{Mn}$  that was  
624 mobilized by water and later precipitated into carbonates, preferentially in the void spaces of  
625 the highly porous parent bodies (Trigo-Rodríguez *et al.*, 2006; Rubin *et al.*, 2007). We found  
626 that dolomite and complex carbonates are developed at the expense of Ca-carbonate in the  
627 highly altered CM chondrites (Rubin *et al.*, 2007; Lee et al., 2014). Extensive aqueous  
628 alteration could also have promoted aqueous flow in the CM parent body producing the lenses  
629 identified in MET 01070 (Trigo-Rodríguez & Rubin, 2006; Rubin *et al.*, 2007, see Fig. 5). It  
630 has been also proposed that the collapse of matrix pore spaces occurred due to shock  
631 propagation associated with impact compaction of the CM and CV parent bodies (Trigo-  
632 Rodríguez et al., 2006; Rubin, 2012). In such circumstances water could have being vaporized  
633 quite quickly leaving the aqueous alteration fronts observed in MET 01070.

634

635 4.2 Atomistic pictures of material/water interfaces relevant for the CCs

636

637 The present work aims to provide proof for the presence of hydrous phases and their  
638 action during the accretion of CCs in the outer regions of the protoplanetary disk. In this section  
639 we synthesise computational chemistry results with quantum mechanical simulations that can  
640 provide atomic-scale information on the interaction of water with materials present in CCs.  
641 Results can in turn can shed some light to the initial steps of water alteration in some minerals  
642 present in CCs.

643



644 Some of the clearest evidence for aqueous alteration is the presence/formation of  
645 phyllosilicates in CCs. Phyllosilicates are also referred to as hydrous silicates because they  
646 incorporate water or hydroxyls. Our recent work on water incorporation has used quantum  
647 chemical calculations (Rimola & Trigo-Rodríguez, 2017), with forsterite ( $\text{Mg}_2\text{SiO}_4$ ) being used  
648 as a silicate test case. In that work, we studied the interaction of 12 water molecules with the  
649 (010), (001) and (110) surfaces of  $\text{Mg}_2\text{SiO}_4$  crystals, which are extended planes in the  $\text{Mg}_2\text{SiO}_4$   
650 crystal structure (as well as with an amorphous surface). It is worth mentioning that these  
651 different  $\text{Mg}_2\text{SiO}_4$  surfaces have contrasting stabilities. The stability of a surface is correlated  
652 with its reactive behavior, and specifically the less stable a surface the greater its reactivity.  
653 The different  $\text{Mg}_2\text{SiO}_4/(\text{H}_2\text{O})_{12}$  systems were geometrically optimized to reach a stable  
654 structure of minimum energy. Figure 9 shows the results obtained. Irrespective of the surface,  
655 water molecules interact with the outermost surface  $\text{Mg}^{2+}$  cations through their O atoms and  
656 also via hydrogen-bond interactions between the O surface atoms of forsterite and the H  
657 protons of water. Moreover, these interactions only occur in the first water layer, whereas the  
658 second water layer was found to be engaged by a H-bond network. However, it was found that  
659 the resulting  $\text{Mg}^{2+}/\text{H}_2\text{O}$  interaction depends on the stability of the silicate surface. For the most  
660 stable surfaces, (010) and the (001), water molecules interacting directly with  $\text{Mg}^{2+}$  are  
661 molecularly adsorbed on the cation; that is, they do not split into  $\text{OH}^+$  H. By contrast, for the  
662 less stable the (110) surfaces and the amorphous surfaces those water molecules interacting  
663 with the  $\text{Mg}^{2+}$  surface cation dissociate whereby one H proton of water is transferred to a nearby  
664 O surface atom, thereby resulting in the formation of Mg-OH and Si-OH surface groups.  
665 Similar results (namely, water dissociation upon  $\text{Mg}_2\text{SiO}_4$  adsorption) were also found by  
666 Priggiobe et al. (2013), in which the  $\text{Mg}_2\text{SiO}_4/\text{H}_2\text{O}$  interface was studied by increasing  
667 progressively the number of water molecules to adsorb. This water dissociation on the most  
668 reactive  $\text{Mg}_2\text{SiO}_4$  surfaces can be interpreted as the first step for the transformation of silicates  
669 into phyllosilicates. In our particular case, formation of chrysotile can take place by hydration  
670 of forsterite; i.e.,  $2\text{Mg}_2\text{SiO}_4 + 3\text{H}_2\text{O} \rightarrow \text{Mg}_3\text{Si}_2\text{O}_5(\text{OH})_4 + \text{Mg}(\text{OH})_2$ .

671  
672 Continuing with the same idea that phyllosilicates are clear evidence for aqueous  
673 alteration during the accretion of CCs, the literature contains a set of computational chemistry  
674 studies based on ab initio molecular dynamic simulations essentially focused on the  
675 dehydroxylation of two phyllosilicates: pyrophyllite (Molina-Montes et al., 2008a; Molina-  
676 Montes et al., 2008b; Molina-Montes et al., 2010) and smectite (Muñoz-Santiburcio et al.,  
677 2012; Muñoz-Santiburcio et al., 2016). These authors identified different competitive paths for  
678 the dehydroxylation of these hydrous minerals, but the major conclusion is that in order to carry  
679 out the reaction high temperatures ( $\approx 1500$  K) are required because of the high activation  
680 energies (about  $60 \text{ kcal mol}^{-1}$  for pyrophyllite and  $50 \text{ kcal mol}^{-1}$  for smectite). This result  
681 indicates that once it has taken place, phyllosilicate dehydroxylation (namely, reverting the  
682 reaction) requires extreme conditions. If this is not the case, then the phyllosilicate remains as  
683 a stable material.

684  
685 The results related to the dissociation of water upon surface interaction also suggest that  
686 in some CCs the presence of iron oxides (and particularly magnetite,  $\text{Fe}_3\text{O}_4$ ) is evidence for

687 alteration by water. We stated above (Section 3.2.2) that iron sulphides, and in particular  
688 pyrrhotite (a nonstoichiometric form of FeS), can be replaced by magnetite during aqueous  
689 alteration. Several theoretical works address the interaction of water with iron sulphide  
690 surfaces. Stirling et al. (2003) studied the interaction of water with the (100) surface of pyrite  
691 (FeS<sub>2</sub>). Results of this work indicated that the most stable FeS<sub>2</sub>/H<sub>2</sub>O structure is that in which  
692 all the water molecules are molecularly adsorbed on the outermost Fe cations. However, the  
693 authors also identified a metastable structure in which some water molecules are in their  
694 dissociated state as a consequence of a proton transfer from H<sub>2</sub>O interacting with Fe to a S  
695 atom, thus resulting in the formation of Fe-OH and S-H surface groups (see Figure 10a).  
696 Remarkably, dissociated water is stabilized by the H-bond interactions established with the rest  
697 of water molecules present in the interface. In absence of water in excess, the dissociative state  
698 is unstable and evolves towards molecular water. Another interesting work is that of Dzade et  
699 al. (2016), where the adsorption of water on a clean and oxygen-covered (011) surface of  
700 mackinawite (a FeS-type mineral) was studied. Results showed that, on the clean surfaces  
701 (namely, in absence of other co-adsorbents), water dissociation is endothermic from its  
702 molecularly adsorbed state (see Figure 10b). However, in the presence of a preadsorbed oxygen  
703 atom on a Fe site (namely, oxygen-covered surface), water dissociation is feasible since a  
704 spontaneous proton transfer reaction from water to the preadsorbed O atom was observed, thus  
705 forming two Fe<sup>3+</sup>-OH<sup>-</sup> ferric hydroxide groups (see Figure 10c). The fact that H<sub>2</sub>O can be  
706 dissociated upon Fe interaction opens up a route towards the formation of iron oxides in the  
707 presence of water. Indeed, in common with silicates, water dissociation on iron sulphides is a  
708 way to incorporate O into the mineral structure, leading to its oxidation. Obviously, taking into  
709 account only the water dissociation process we cannot explain the full iron sulphide → iron  
710 oxide conversion process. Other intriguing aspects remain to be answered such as removal of  
711 the surface H atoms (originating from water), the growth of the iron oxide, and the need or  
712 otherwise of co-adsorbents activating the process. This water dissociation phenomenon,  
713 however, allows us to determine the initial steps towards the formation of iron oxides from iron  
714 sulphides.

715  
716 Another interesting point is the mobilization of certain elements due to the action of  
717 water. Water can play a major role in the diffusion and migration of elements (particularly in  
718 the form of cations such as Na<sup>+</sup>), thus altering the composition of the CC materials. A nice  
719 theoretical work demonstrating the capability of water in mobilizing metal cations is that of  
720 Mignon et al. (2010). These authors used ab initio molecular dynamics simulations to explore  
721 the fate of Li<sup>+</sup>, Na<sup>+</sup> and K<sup>+</sup> bound on the surfaces of the interlayer regions on montmorillonite  
722 clays under wet conditions. Results indicated that K<sup>+</sup> cations remain attached to the interlayer  
723 surfaces. In contrast, Li<sup>+</sup> cations are hydrated by four water molecules, thus trapping them and  
724 removing them from the interlayer surfaces. Na<sup>+</sup> cations show an intermediate behavior:  
725 whether or not they become hydrated depends on the position they occupy in the interlayer  
726 region. (Mignon et al., 2010) found a correlation of their results with the water-cation and  
727 surface-cation affinities. That is, the binding affinity of the alkali cations with water followed  
728 Li<sup>+</sup> > Na<sup>+</sup> > K<sup>+</sup>, while their interaction with the interlayer surfaces follow the sequence of (from  
729 less to more favorable) Li<sup>+</sup> < Na<sup>+</sup> < K<sup>+</sup>. These results provide atomic-scale evidence for the

730 potential role of water in trapping and sequestering certain metal cations placed on the  
731 outermost positions of the materials, thus favoring their mobility and migration to other  
732 positions as clear effect of water alteration.

733

## 734 **5. Conclusions**

735

736 In view of current evidence, the CCs contain highly reactive minerals that have been  
737 continuously reaching the terrestrial surface, although the flux has significantly changed over  
738 time (Trigo-Rodríguez et al., 2017). The study of the highly unequilibrated materials forming  
739 these meteorites reveals that they formed part of undifferentiated parent bodies accreted in the  
740 outer protoplanetary disk, and their composition reinforces the idea of a continuum between  
741 asteroids and comets. These bodies formed from primordial protoplanetary disk materials, and  
742 at the very beginning were subjected to planetary perturbations, collisions with other bodies  
743 and fragmentations during close approaches to planets so probably they were easily disrupted  
744 (Trigo-Rodríguez and Blum, 2009; Trigo-Rodríguez, 2015). The delivery of these materials to  
745 terrestrial planets increased during the Late Heavy Bombardment (Gomes et al., 2005).  
746 Consequently, it seems plausible that at early times and subsequent ulterior periods of time the  
747 Earth was subjected to a meteoritic flux at least 5-6 orders of magnitude greater than the current  
748 one (Trigo-Rodríguez et al., 2004) that has been estimated to be ~40,000 Tm/year (Brownlee,  
749 2001). Consequently, we predict that a large amount of chondritic materials reached the early  
750 Earth's surface at an annual rate of thousands of billions of metric tons. Hence the amount of  
751 volatiles and catalytic minerals delivered under such meteoroid high-flux circumstances was  
752 also very significant, probably playing a key role in fertilizing the Earth's surface (Rotelli et  
753 al., 2016). As consequence of our present study we have reached the following conclusions:

754

755 - We have presented evidence for aqueous alteration in carbonaceous chondrites that can be  
756 explained by the incorporation of hydrated materials into the fine-grained matrix. As their  
757 parent bodies were compacted by collisional processing and self-gravity, only those that  
758 escaped significant metamorphism or aqueous alteration can provide direct clues needed  
759 to understand the delivery of water to terrestrial planets.

760

761 - Many carbonaceous chondrites contain valuable chemical, isotopic and mineralogical  
762 information on the nebular environment, but exhibit densities and porosities different to  
763 their precursor materials. The effects of aqueous alteration and impact metamorphism  
764 make finding undifferentiated bodies preserving primordial physical properties a difficult  
765 task, but meteorites such as ALHA77307 and Acfer 094 shows that they do exist (Rubin  
766 *et al.*, 2007; Trigo-Rodríguez & Blum, 2009a). Sample-return missions from the future  
767 exploration of ice-rich bodies stored among the Centaurs or Kuiper Belt populations will  
768 provide new clues and answers.

769

770 - Carbonaceous chondrites are the legacy of the first accretionary stages of our  
771 protoplanetary disk. Accretion of abundant organic- and ice-rich phases occurred behind  
772 the so-called snow line, so in the outer disk distinctive materials were available to form

773 transitional bodies. The recognized progenitors of these primitive meteorites are volatile-  
774 rich asteroids, and comets. To explain the current O-isotopic evidence, our current  
775 formation scenario indicates that Jupiter precluded significant inward transport of outer  
776 disk comets, being probably the cause for the two distinguishable sources of water  
777 identified so far. The outer border of the inner disk where the CCs mostly incorporated  $^{16}\text{O}$ -  
778 rich water, while the  $^{16}\text{O}$ -poor signature seems to be characteristic of outer disk water ice  
779 hosted by cometary materials.

780

781 - *Transitional* bodies probably accreted not only anhydrous minerals, but also significant  
782 amounts of ice, hydrated minerals, and organic materials that made them highly porous in  
783 the very beginning. These materials accreted as very small grains, or attached to other  
784 phases forming meteorite matrices. Ices and organics could have helped to bind the  
785 primordial dust aggregates without the need for significant compaction.

786

787 - Carbonaceous chondrites formed from outer disk aggregates containing variable ice/rock  
788 ratios. Radiogenic elements (e.g.  $^{26}\text{Al}$ ,  $^{60}\text{Fe}$ ) were incorporated from the stellar  
789 environments from which our planetary system formed. Then, once consolidated,  
790 radiogenic decay probably provided the heat required to release enough water for aqueous  
791 alteration during the first 10 Ma after accretion. Mineralogical evidence, mostly formation  
792 and dating of carbonates, indicates that aqueous alteration and outgassing transformed  
793 these bodies at that early stage, thus being consistent with radiogenic decay.

794

795 - The brecciated nature, deformation and lineation of some components contained in CCs  
796 suggest that shock produced by stochastic collisions was an additional source of heat that,  
797 due to the relatively limited abundance of water, mostly promoted static aqueous  
798 alteration.

799

800 - Atomistic simulations based on computational chemistry methods are potential powerful  
801 tools for providing atomic-scale insights into water-mediated alteration of minerals present  
802 in CCs. The simulations provide a comprehensive understanding of the first steps for the  
803 conversion of anhydrous silicates into phyllosilicates, the oxidation (namely, incorporation  
804 of O) of iron sulfides, and the mobility of metal cations present at the mineral surfaces

805

806 Concerning future work we consider that it is urgent to perform radiogenic dating of  
807 some more of the aqueous alteration products in order to reconstruct the sequence of events  
808 involved in the alteration of the parent bodies of CM and CR chondrites. Some meteorites have  
809 being studied, but still we lack measurements dating these pre-accretionary minerals described  
810 in this work. These studies are of key importance to establish the pathway of delivery of  
811 volatiles to the terrestrial planets.

812

813

814

815

## Acknowledgements

We thank two anonymous reviewers that improved significantly this manuscript. Spanish Ministry of Science and Innovation under research projects AYA2015-67175-P and CTQ2017-89132-P are acknowledged, and we also thank the UK Science and Technology Facilities Council for funding through project ST/N000846/1. Mike Zolensky is acknowledged for kindly providing the Murchison and Renazzo pristine sections studied in this work. AR is indebted to “Ramón y Cajal” program. ST made this study in the frame of a PhD. on Physics at the Autonomous University of Barcelona (UAB). M. del Mar Abad is acknowledged by her interpretation of the data obtained of Murchison CM2 using the HR-TEM image (Fig. 4) obtained by JMTR at Centro de Instrumentación Científica (CIC), Universidad de Granada.

## REFERENCES

- Abreu N.M. and Brearley, A.J. *Geoch. Cosm. Acta* 74, 1146 (2010)
- Alexander, C.M.O'D., McKeegan, K.D. and Altwegg, K. *Space Sci. Rev.* 214: 36 (2018)
- Alexander, C.M.O'D., G.D. Cody, B.T. De Gregorio, L.R. Nittler, and R.M. Stroud. *Chemie der Erde* 77, 227 (2017)
- Amelin, Y., Krot, A.N., Hutcheon, I.D., & Ulyanov, A.A. *Science*, 297, 1678 (2002)
- Anders, E. and Grevese, N. *Geoch. Cosmoch. Acta*, 53, 197 (1989)
- Armitage P.J. *Annu. Rev. Astron. Astrophys.*, 49, 195 (2011)
- Beitz, E., Güttler, C., Nakamura, A. M., Tsuchiyama, A. & Blum, J. *Icarus*, 225, 558 (2013)
- Beitz, E., Blum, J., Parisi, M. G., and Trigo-Rodriguez, J. *Ap.J.* 824:1, article id. 12 (2016)
- Bischoff, A. *Meteorit. Planet. Sci.* 33, 1113 (1998)
- Bischoff, A., Scott, E.R.D., Metzler, K. & Goodrich, C.A. In *Meteorites and the Early Solar System II*, D.S. Lauretta & H.Y. McSween, eds. (The University of Arizona Press, Tucson, 2006), pp.679-712
- Bland, P. A., Collins, G. S., Davison, T. M., Abreu, N. M., Ciesla, F. J., Muxworthy, A. R., and Moore, J. *Nature Communications* 5, id. 5451 (2014)
- Blum, J., Schräpler, R., Davidson, B.J.R. & Trigo-Rodríguez, J.M. *Ap J.* 652, 1768 (2006).
- Boss A.P. *Ap.J.* 764, 194 (2013)

859 Brearley, A.J. *Science* 276, 1103-1105 (1997)  
860  
861 Brearley, A. J. and Jones, R.H. In *Planetary Materials*, J.J. Papike, ed., *Reviews in Mineralogy*,  
862 36, Mineralogical Society of America, Washington, 1998), pp-1-398 (1998)  
863  
864 Brearley A. J. In *Meteorites and the Early Solar System II*, ed. D. S. Lauretta and H. Y.  
865 McSween, (Univ. Arizona Press, Tucson, 2006), pp. 587-624 (2006)  
866  
867 Briani, G., Morbidelli, A., Gounelle, M., and Nesvorný, D. *Meteoritics & Planetary Science*  
868 46, 1863 (2011)  
869  
870 Browning L., McSween H. and Zolensky M. *Geochim. Cosmochim. Acta* 60, 2621 (1996)  
871  
872 Brownlee D.E. In *Accretion of Extraterrestrial Matter Throughout Earth's history*. B. Peucker-  
873 Ehrenbrink and B. Schmitz (eds.), Kluwer Academic/Plenum Publishers, New York,  
874 USA, pp. 1-12 (2001)  
875  
876 Brownlee D., et al. *Science* 314, 1711 (2006)  
877  
878 Busemann, H. Young, A.F., Alexander, C.O'D., Hoppe, P., Mukhopadhyay, S., Nittler, L.R..  
879 *Science* 312, 727 (2006).  
880  
881 Carporzen L., Weiss, B.P., Elkins-Tanton, L.T., Shuster, D.L., Ebel, D. and Gattacceca, J. *Proc.*  
882 *National Academy Sciences* 108, 6386 (2011)  
883  
884 Cliff G. and Lorimer G.W. *J. Microscopy* 103, 203 (1975)  
885  
886 Dobrică, E., Brearley, A. J. *Meteoritics & Planetary Science*, 49, 1323 (2014)  
887  
888 Doyle, P.M., Jogo, K., Nagashima, K., Krot, A.N., Wakita, S., Ciesl, F.J., and Hutcheon, I.D.  
889 *Nature Communications*, doi: 10.1038/ncomms8444 (2015)  
890  
891 Dzade, N.Y., Roldan, A.. de Leeuw, N.H. (2016) *J. Phys. Chem. C*, 120, 21441–21450.  
892  
893 Dyl, K.A., Bischoff, A., Ziegler, K., Young, E.D., Wimmer, K. and Bland, P.A. *Proceedings*  
894 *of the National Academy of Sciences*, 109, 18306 (2012)  
895  
896 Endreß, M. & Bischoff, A. *Geochimica & Cosmochimica Acta*, 60, 489 (1996)  
897  
898 Fegley, B., Jr. and Prinn, R.G. In *The Formation and Evolution of Planetary Systems*, Space  
899 Telescope Science Institute Symposium Series, H.A. Weaver and L. Danly (eds.) (1989)  
900

901 Fuchs L. H., Olsen E., and Jensen K. J. *Smithsonian Contributions to Earth Science* 10:39  
902 (1973)  
903  
904 Fuente, A., Cernicharo, J., Roueff, E., Gerin, M., Pety, J., Marcelino, N., Bachiller, R.,  
905 Lefloch, B., Roncero, O., and Aguado, A. *Astronomy and Astrophysics* 593, A94 (2016)  
906 Garenne, A., Beck, P., Montes-Hernandez, G., Chiriac, R., Toche, F., Quirico, E., Bonal, L.,  
907 and Schmitt, B. *Geochimica et Cosmochimica Acta* 137, 93 (2014)  
908  
909 Gomes R., Levison H. F., Tsiganis K., Morbidelli A. Origin of the cataclysmic Late Heavy  
910 Bombardment period of the terrestrial planets. *Nature* 435, 466 (2005)  
911  
912 Hanna, R.D., Ketcham, R.A., Zolensky, M., Behr, W.M. *Geochimica et Cosmochimica Acta*  
913 171, 256 (2015)  
914  
915 Hanowski N. P. and Brearley A. J. *Meteorit. Planet. Sci.* 35, 1291 (2000)  
916  
917 Howard, K.T., Alexander, C.M.O'D, Schrader, D.L., and Dyl, K.A. *Geochim. Cosmochim.*  
918 *Acta* 149, 206 (2015)  
919  
920 Hutchison R. *Meteorites*, Cambridge Univ. Press, 506 pp. (2004)  
921  
922 Jewitt, D., Chizmadia, L., Grimm, R. and Prrialnik, D. In *Protostars and Planets V*, B. Reipurth,  
923 D. Jewitt and K. Keil (eds.), Univ. Arizona Press, pp. 863-867 (2007)  
924  
925 King, A.J., Schofield, P.F., and Russell, S.S. *Meteoritics and Planetary Science* 52, 1197 (2017)  
926  
927 Le Guillou, C., and Brearley, A.J. *Geochimica et Cosmochimica Acta* 131, 344 (2014)  
928  
929 Le Guillou, C., Changela, H.G., Brearley, A.J. (2015) *Earth and Planetary Science Letters* 420,  
930 162 (2015)  
931  
932 Kunihiro T., Rubin, A.E., McKeegan, K.D. and Wasson, J.T. *Geochimica Cosmochimica Acta*  
933 68, 3599 (2004)  
934  
935 Lee, M.R., Lindgren, P., Sofe, M.R., O'D Alexander, C.M. & Wang, J. *Geochimica*  
936 *Cosmochimica Acta*, 92, 148 (2012).  
937  
938 Lee, M.R. and Lindgren, P. *Meteoritics and Planetary Science* 51, 1003 (2016)  
939  
940 Lee, M.R., Lindgren, P. and Sofe, M.R. *Geochimica et Cosmochimica Acta* 144, 126 (2014)  
941  
942 Lindgren, P., Hanna, R.D., Dobson, K.J., Tomkinson, T. and Lee, M.R. *Geochimica et*  
943 *Cosmochimica Acta* 148, 159-178. (2015)  
944  
945 Lodders, K. *The Astrophysical Journal* 591, 1220 (2003)

946  
947 Lodders, K. and Fegley, B. In *Chemistry of the Solar System*, RSC Publishers, ISBN: 978-0-  
948 85404-128-2, 496 pp. (2011)  
949  
950 Lodders, K. and Amari S. *Chemie der Erde* 65, 93–166 (2005)  
951  
952 Lorimer G.W. and Cliff G. (1976) In *Electron Microscopy in Mineralogy*, Ed. by H. R.  
953 Wenk, Berlin Springer-Verlag, Berlin, 506 (1976)  
954  
955 Marchi, S., Delbó, M., Morbidelli, A., Paolicchi, P., and Lazzarin, M. *Monthly Notices of the*  
956 *Royal Astronomical Society* 400, 147 (2009)  
957  
958 Marrocchi, Y., Bekaert, D.V. and Piani, L. *Earth Planet. Sci. Lett.* 482, 23 (2018)  
959  
960 Martins, Z., Alexander, C. M. O'D., Orzechowska, G. E., Fogel, M. L., and Ehrenfreund, P.  
961 *Meteoritics & Planetary Science* 42, 2125 (2007)  
962  
963 Mignon, P., Ugliengo, P., Sodupe, M., Hernandez, E.R. (2010): Ab initio molecular dynamics  
964 study of the hydration of Li<sup>+</sup>, Na<sup>+</sup> and K<sup>+</sup> in a montmorillonite model. Influence of  
965 isomorphic substitution. *Phys. Chem. Chem. Phys.*, 12, 688–697.  
966  
967 Molina-Montes, E., Donadio, D., Hernández-Laguna, A., Sainz-Díaz, C.I., Parrinello, M.  
968 (2008a): DFT Research on the Dehydroxylation Reaction of Pyrophyllite 1. First-  
969 Principle Molecular Dynamics Simulations. *J. Phys. Chem. B*, 112, 7051–7060.  
970  
971 Molina-Montes, E., Donadio, D., Hernández-Laguna, A., Sainz-Díaz, C.I., (2008b): DFT  
972 Research on the Dehydroxylation Reaction of Pyrophyllite 2. Characterization of  
973 Reactants, Intermediates, And Transition States along the Reaction Path. *J. Phys.*  
974 *Chem. A*, 112, 6373–6383.  
975  
976 Molina-Montes, E., Donadio, D., Hernández-Laguna, A., Sainz-Díaz, C.I., (2010): Exploring  
977 the Rehydroxylation Reaction of Pyrophyllite by Ab Initio Molecular Dynamics. *J.*  
978 *Phys. Chem. B*, 114, 7593–7601.  
979  
980 Moyano-Camero, C. E., Nittler, L. R., Trigo-Rodríguez, J. M., Alexander, C. M. O'D.,  
981 Davidson, J., and Stroud, R. M. 47th Lunar and Planetary Science Conference, LPI  
982 Contribution No. 1903, p.2537 (2016)  
983  
984 Muñoz-Santiburcio, D., Kosa, M., Hernández-Laguna, A., Sainz-Díaz, C.I., Parrinello, M.  
985 (2012): Ab Initio Molecular Dynamics Study of the Dehydroxylation Reaction in a  
986 Smectite Model. *J. Phys. Chem. C*, 116, 12203–12211.  
987



988 Muñoz-Santiburcio, D., Hernández-Laguna, A., Sainz-Díaz, C.I. (2016): Simulating the  
989 Dehydroxylation Reaction in Smectite Models by Car–Parrinello-like-Born-  
990 Oppenheimer Molecular Dynamics and Metadynamics. *J. Phys. Chem. C*, 120,  
991 28186–28192.  
992  
993 Nittler L.R., Trigo-Rodríguez, J.M. Stroud, R.M., De Gregorio, B.T., Alexander, C.M.O'D.,  
994 Davidson, J., Moyano-Camero, C.E., and Tanbakouei, S. Nature Communications,  
995 submitted, (2019)  
996  
997 Piani, L., Yurimoto, H. and Remusat, L. (2018) Nature Astronomy 2, 317 (2018)  
998  
999 Prigobbe, V., Suarez Negreira, A., Wilcox, J. (2013): Interaction between Olivine and Water  
1000 Based on Density Functional Theory Calculations. *J. Phys. Chem. C*, 117, 21203–  
1001 21216.  
1002  
1003 Rimola, A., Trigo-Rodríguez, J.M. (2017): Atomistic Simulations of Aqueous Alteration  
1004 Processes of Mafic Silicates in Carbonaceous Chondrites. Pp. 103-127 in: *Assessment*  
1005 *and Mitigation of Asteroid Impact Hazards* (J.M. Trigo-Rodríguez, M. Gritsevich & H.  
1006 Palme, editors). Astrophysics and Space Science Proceedings 46, Springer, Cham,  
1007 Switzerland.  
1008  
1009 Rotelli L., Trigo-Rodríguez, J.M., Moyano-Camero, C.E., Carota, E., Botta, L., Di Mauro,  
1010 E., y Saladino R., The key role of meteorites in the formation of relevant prebiotic  
1011 molecules in a formamide/water environment. Nature Sci. Rep. 6, Article number:  
1012 38888 (2016)  
1013  
1014 Rubin, A.E. Meteoritics and Planetary Science 32, 231 (1997)  
1015  
1016 Rubin, A.E. Geochimica Cosmochimica Acta, 68, 673 (2004)  
1017  
1018 Rubin, A.E. Geochimica Cosmochimica Acta, 90, 181 (2012)  
1019  
1020 Rubin, A., Trigo-Rodríguez, J.M., Huber, H. & Wasson, J.T. Geoch. Cosm. Acta, 71, 2361  
1021 (2007)  
1022  
1023 Schrader D.L., Connolly Jr. H.C., Laurretta D.S., Nagashima K., Huss G.S, Davidson J.,  
1024 Domanik K.J. Geoch. Cosmoch. Acta, 101, 302 (2013)  
1025  
1026 Schulz R., Hilchenbach, M., Langevin, Y., Kissel, J., Silen, J. et al. Nature 518, 216 (2015)  
1027  
1028 Shah, J., Bates, H.C., Muxworthy, A. R., Hezel D.C., Russell, S.S., and Genge M.J. Earth and  
1029 Planetary Science Letters 475, 106 (2017)  
1030

1031 Singerling, S.A. and Brearley, A.J. *Meteoritics and Planetary Science*, doi:  
1032 10.1111/maps.13108, 29 pp. (2018)  
1033  
1034 Stirling, A., Bernasconi, M., Parrinello, M. *J. Chem. Phys.*, 118, 8917 (2003)  
1035  
1036 Stroud, R. M., Nittler, L. R., Moyano-Camero, C. E., Trigo-Rodríguez, J. M., Davidson, J.,  
1037 De Gregorio, B. T., and Alexander, C. M. O'D. 79th Annual Meeting of the  
1038 Meteoritical Society, LPI Contribution No. 1921, id.6360 (2016)  
1039  
1040 Takir, D., Emery, J.P., McSween, H.Y., Hibbitts, C.A., Clark, R.N., Pearson, N., Wang, A.  
1041 *Meteoritics & Planetary Science* 48, 1618 (2013)  
1042  
1043 Trigo-Rodríguez, J.M. In *Planetary Materials*, Edited by M.R. Lee and H. Leroux, 301 pp.,  
1044 ISBN:978-0903056-55-7, Published by the European Mineralogical Union and the  
1045 Mineralogical Society of Great Britain and Ireland, p. 67 (2015)  
1046  
1047 Trigo-Rodríguez, J.M. and Blum, J. *Planetary and Space Science* 57, 243 (2009)  
1048  
1049 Trigo-Rodríguez, J.M., Rubin, A.E. and Wasson, J.T. *Geoch. Cosmoch. Acta*, 70, 1271  
1050 (2006)  
1051  
1052 Trigo-Rodríguez, J. M.; Llorca, J.; Oró, J. In *Life in the Universe: From the Miller*  
1053 *Experiment to the Search for Life on Other Worlds*. Edited by J. Seckbach, J. Chela-  
1054 Flores, T. Owen, and F. Raulin. 387 pp., ISBN 1-4020-2371-5 (HB), Published by  
1055 Springer, Berlin, 2004, p.201 (2004)  
1056  
1057 Trigo-Rodríguez, J. M., Delbó, M., and Blum, J. European Planetary Science Congress 2009,  
1058 held 14-18 September in Potsdam, Germany, p. 520 (2009)  
1059  
1060 Trigo-Rodríguez, J.M., Moyano-Camero, C.E., Mestres, N., Fraxedas, J., Zolensky, M.E.,  
1061 Nakamura, T. & Martins, Z. In 44th Lunar and Planetary Sciences Conference, abstract  
1062 #1929 (2013)  
1063  
1064 Trigo-Rodríguez, J. M.; Vila-Ruaix, A.; Alonso-Azcárate, J.; Abad, M. M. In *Highlights on*  
1065 *Spanish Astrophysics IX, Proceedings of the XII Scientific Meeting of the SEA*, S.  
1066 Arribas et al. (eds.), pp. 531-542 (2017)  
1067  
1068 Velbel M. A. and Palmer E. E. *Clays and Clay Minerals* 59, 416 (2011)  
1069  
1070 Velbel M. A., Tonui E. K., and Zolensky M. E. *Geochimica et Cosmochimica*  
1071 *Acta* 87, 117 (2012)  
1072  
1073 Wasson, J.T., and Rubin A.E. *Geoch. Cosmoch. Acta*, 74, 2212 (2010)

1074  
1075 Weisberg M.K., McCoy T.J. & Krot A.N. In *Meteorites and the Early Solar System II*, D.S.  
1076 Lauretta & H. Y. McSween, eds.. (The University of Arizona Press, Tucson, 2006) pp.  
1077 19-52.  
1078  
1079 Zhang K, Blake G.A., and Bergin E.A. *Astrophysical Journal Lett.* 806, art. Id. L7, 6 pp. (2015)  
1080  
1081 Zinner E. In *Treatise on Geochemistry*, Volume 1. Editor: Andrew M. Davis. Executive  
1082 Editors: Heinrich D. Holland and Karl K. Turekian. ISBN 0-08-043751-6. Elsevier, p.17-39  
1083 (2003)  
1084  
1085 Zolensky, M.E. & McSween H. Jr. In: *Meteorites and the Early Solar System* (J.F. Kerridge &  
1086 M.S. Matthews, editors). pp. 114–143. The University of Arizona Press, Tucson, AZ, USA  
1087 (1988).  
1088  
1089 Zolensky, M.E., Barret, T. & Browning, L. *Geochimica Cosmochimica Acta*, 57, 3123 (1993)  
1090  
1091 Zolensky, M. E. & Ivanov, A. *Chemie der Erde*, 63, 185 (2003)  
1092  
1093 Zolensky, M.E., Krot, A.N., Benedix, G. Record of low-temperature alteration in asteroids.  
1094 Pp. 429–462 in: *Oxygen in the Solar System* (G.J. MacPherson, D.W. Mittlefehldt, J.H. Jones  
1095 & S.B. Simon, editors). *Reviews in Mineralogy & Geochemistry*, 68. Mineralogical Society of  
1096 America, Washington, D.C., (2008)  
1097  
1098  
1099  
1100  
1101  
1102  
1103  
1104  
1105  
1106  
1107  
1108  
1109  
1110  
1111  
1112  
1113  
1114  
1115  
1116

1117  
1118  
1119

## TABLES

**Table 1.** Secondary minerals identified in the carbonaceous chondrites

CI	CM	CR	CV/CK	Ungrouped	Mineral Group
Serpentine	Serpentine	Serpentine	Serpentine	Serpentine	<b>Phyllosilicates</b>
Saponite	Chlorite	Saponite	Chlorite	Saponite	
	Vermiculite		Micas		
Magnetite	Magnetite	Magnetite	Magnetite	Magnetite	<b>Oxides</b>
Calcite	Calcite	Calcite	-	-	<b>Carbonates</b>
Dolomite	Dolomite				
Breunnerite	Aragonite				
Siderite					
Apatite	-	-	-	-	<b>Phosphates</b>
Merrillite					
Pyrrhotite	Pyrrhotite	Pyrrhotite	Pyrrhotite	-	<b>Sulphides</b>
Pentlandite	Pentlandite	Pentlandite	Pentlandite		
Cubanite	Tochilinite				
Sulfur	Awaruite				
-	Brucite	-	-	-	<b>Hydroxides</b>
	Tochilinite				
-	Halite	-	-	-	<b>Halides</b>

1120 See also Rubin (1997), Trigo-Rodríguez *et al.* (2006) and Takir *et al.* (2013)

1121

1122 Table 2. Bulk composition of the aqueously formed lens in the MET 01070 CM2  
1123 chondrite compared with two Murchison aureoles (for more details see Rubin *et al.*, 2007)

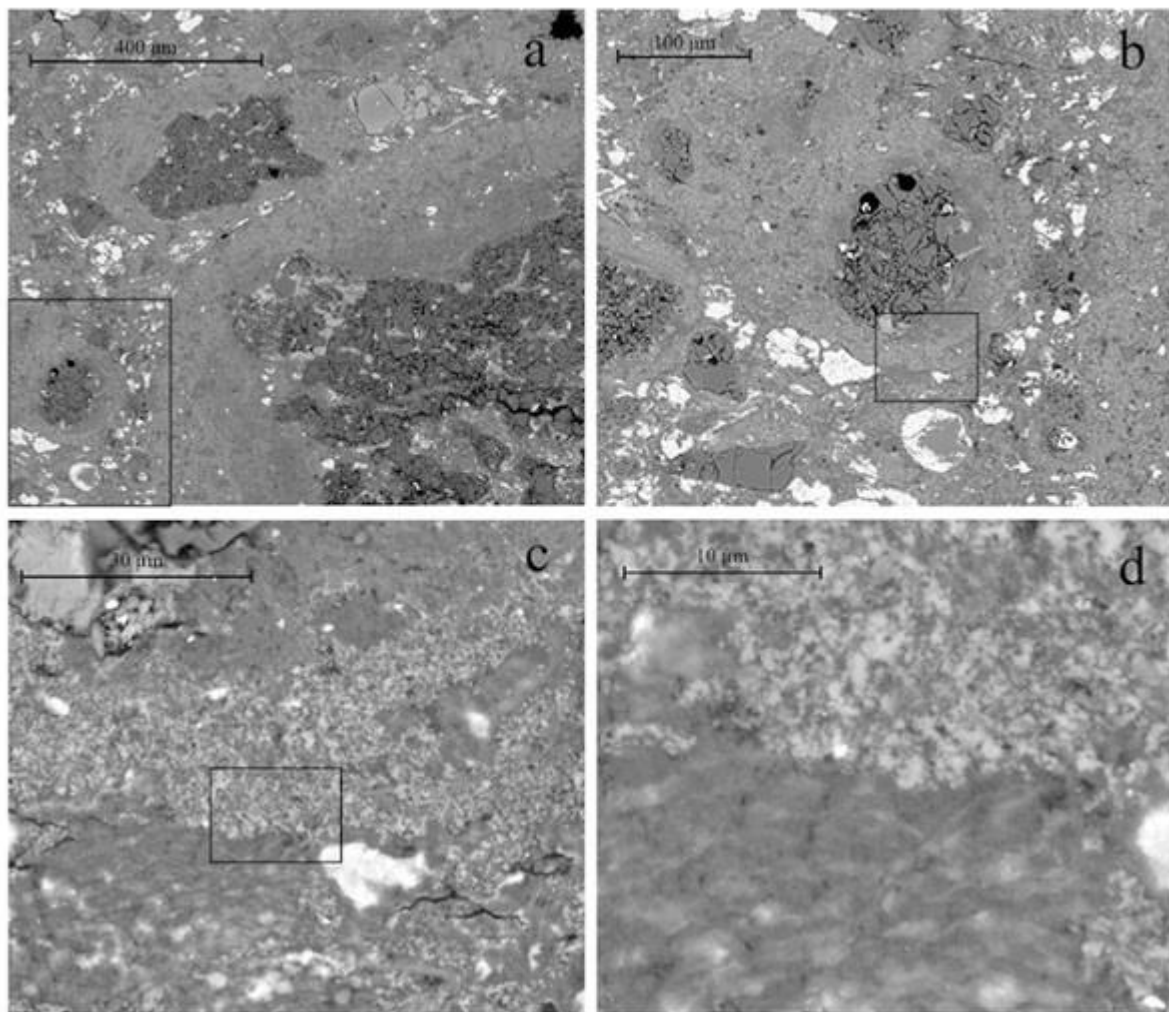
1124

Component	% in MET 01070 lens (n=23)	% in Murchison aureoles (n=2)
SiO <sub>2</sub>	27.0 ± 4.6	5.61
TiO <sub>2</sub>	0.10 ± 0.06	0.16
Al <sub>2</sub> O <sub>3</sub>	2.5 ± 0.38	2.0
FeO	35.8 ± 3.5	43.6
Cr <sub>2</sub> O <sub>3</sub>	0.42 ± 0.18	6.1
MnO	0.25 ± 0.04	0.23
MgO	16.4 ± 2.2	6.7
CaO	0.15 ± 0.12	0.3
Na <sub>2</sub> O	0.20 ± 0.03	0.23
K <sub>2</sub> O	<0.04 ± 0.01	-
P <sub>2</sub> O <sub>5</sub>	<0.04 ± 0.04	-
NiO	0.72 ± 0.44	7.6
S	1.5 ± 0.97	8.3

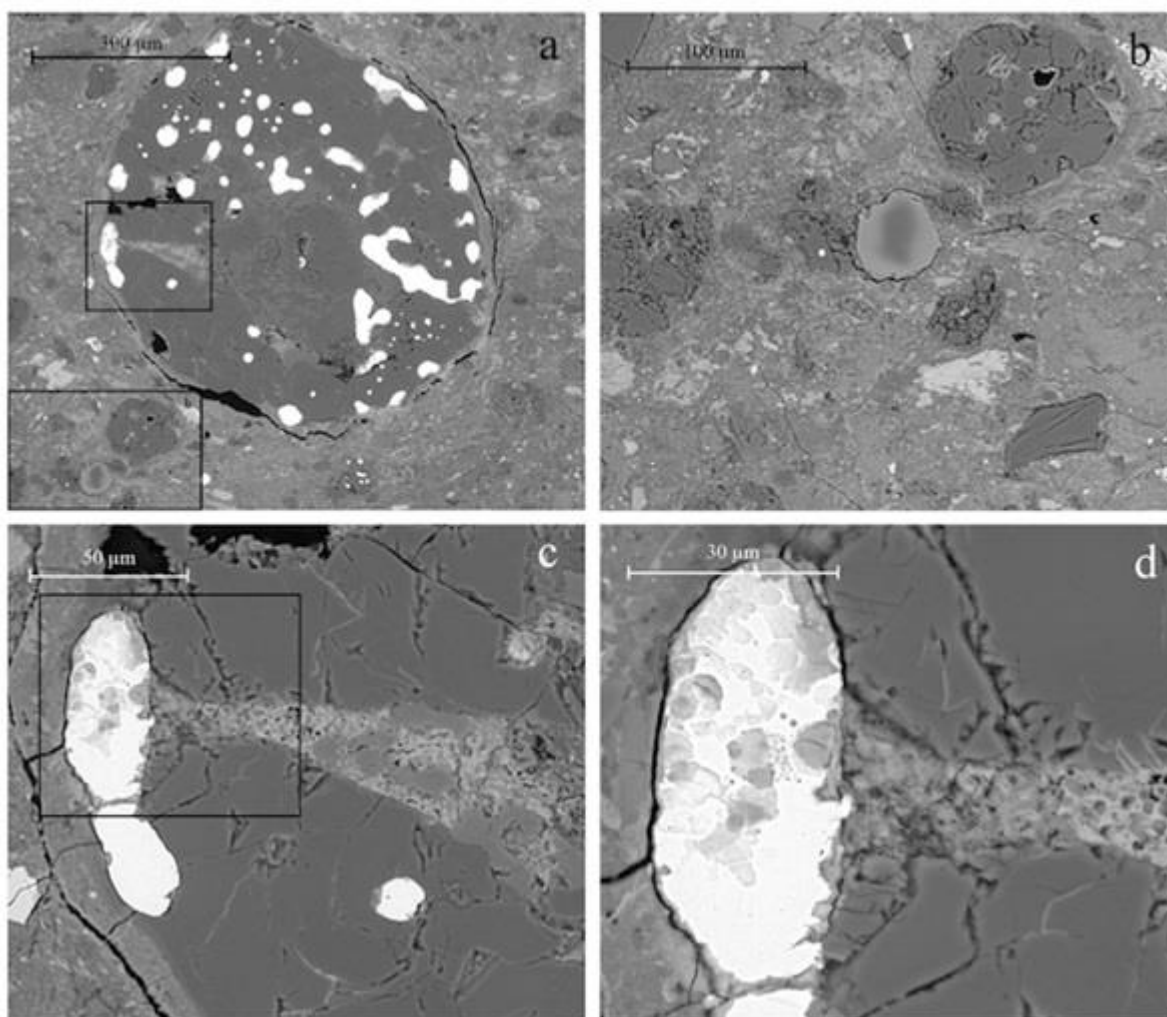
1125

1126  
1127

## FIGURES

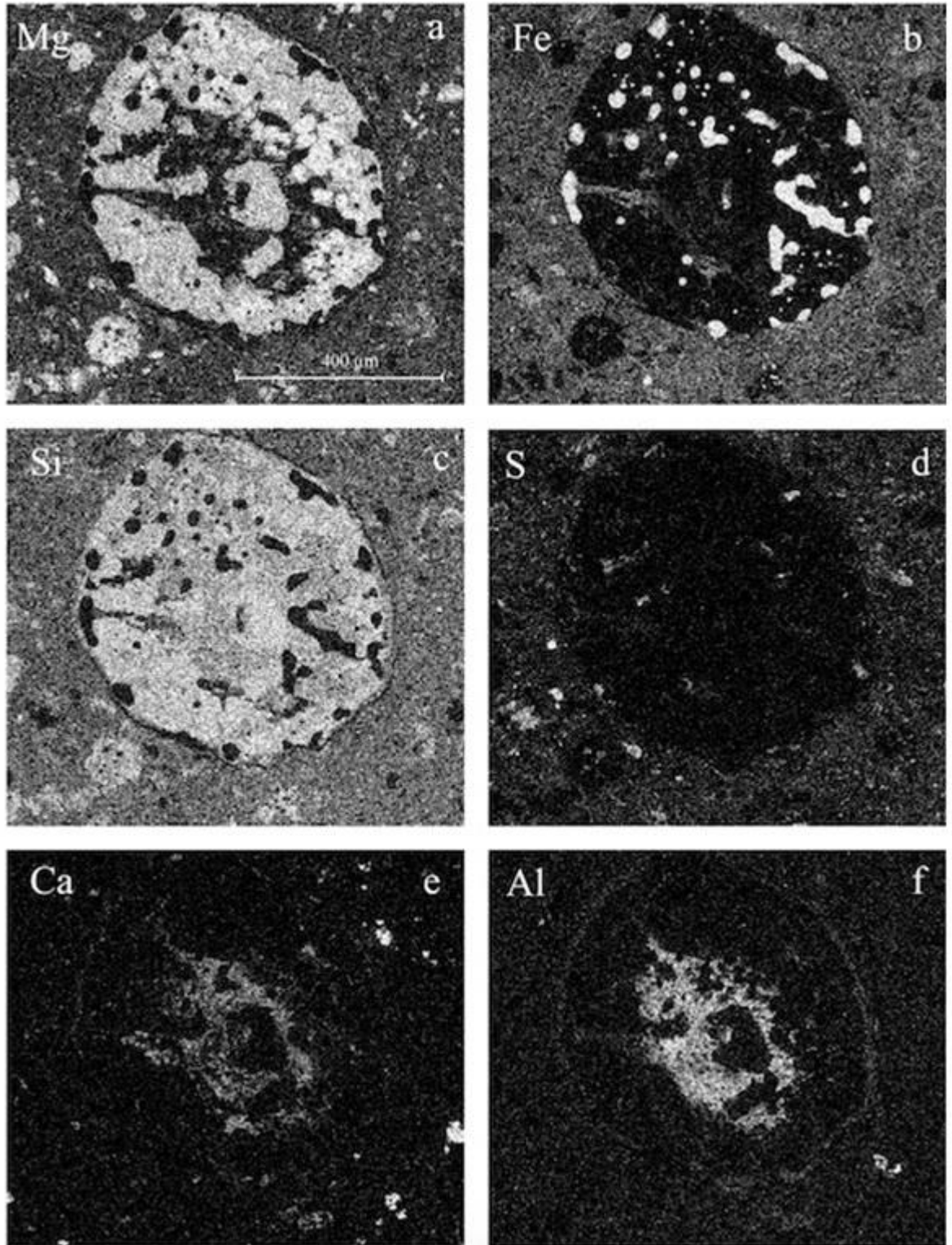


1128  
1129 Figure 1. A zoom-in sequence of BSE images of a thin section of the Murchison CM2 chondrite  
1130 that focuses on three chondrules and the texture of the mantles and surrounding matrix. a)  
1131 Image showing the fine matrix texture, together with chondrules, and fragments. b) The lower  
1132 left chondrule exhibits its own mantle and the different texture is highlighted at higher  
1133 magnifications in c), and d).  
1134  
1135  
1136  
1137  
1138  
1139



1141  
1142 Figure 2. BSE images of a chondrule in the Murchison CM2 chondrite. (a) The metal-rich  
1143 chondrule with two areas of interest framed. In (b) there is a relict grain while in (c) and (d) the  
1144 metal grain is magnified in order to show how water corroded it and penetrates inside the  
1145 chondrule.

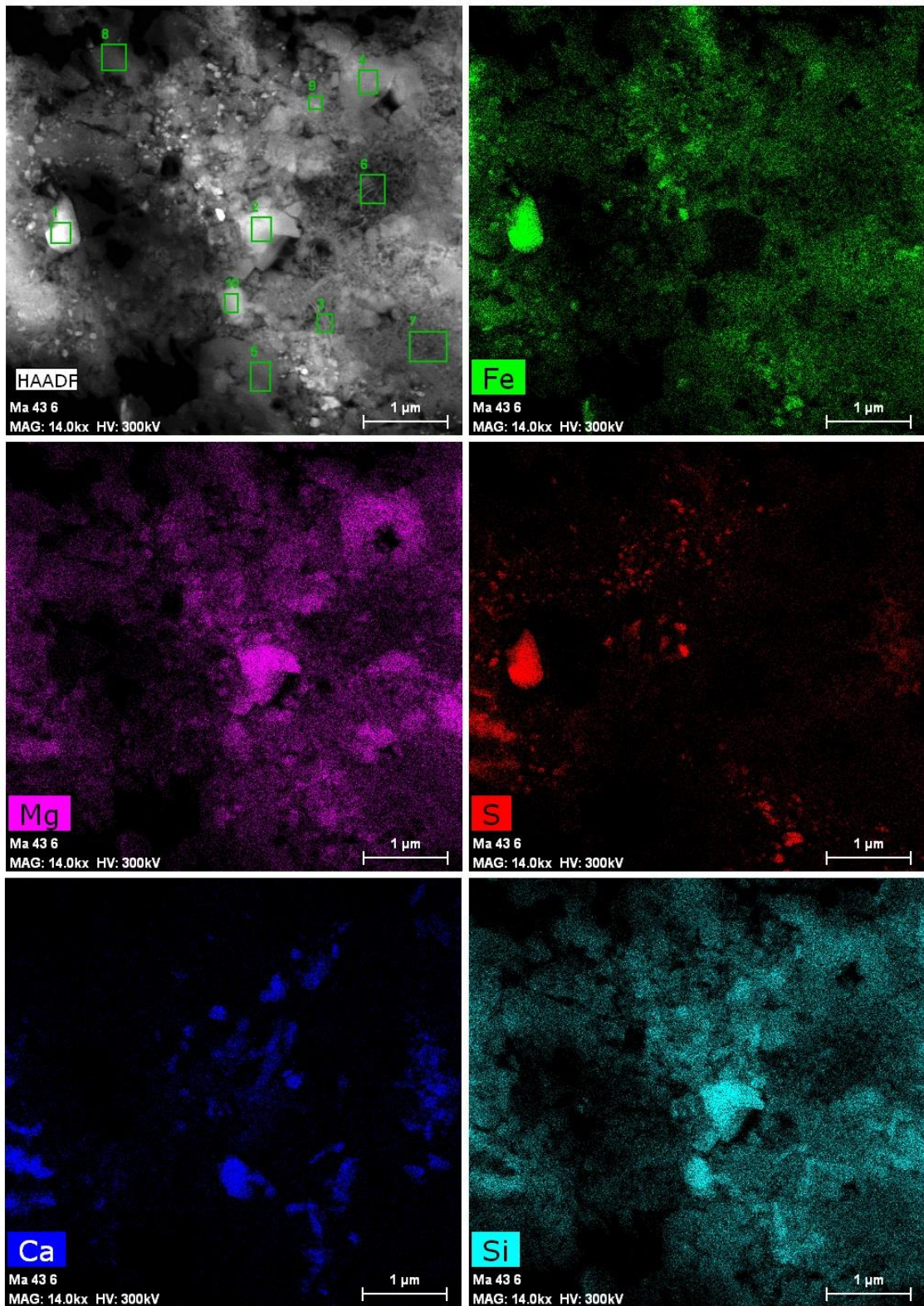
1146  
1147  
1148  
1149  
1150  
1151  
1152  
1153  
1154  
1155  
1156  
1157



1158  
1159  
1160  
1161  
1162  
1163  
1164

Figure 3. X-ray images of the chondrules described in Fig. 2 where the relative abundance of Mg, Fe, Si, S, Ca and Al in the rock-forming minerals is a function of their brightness.





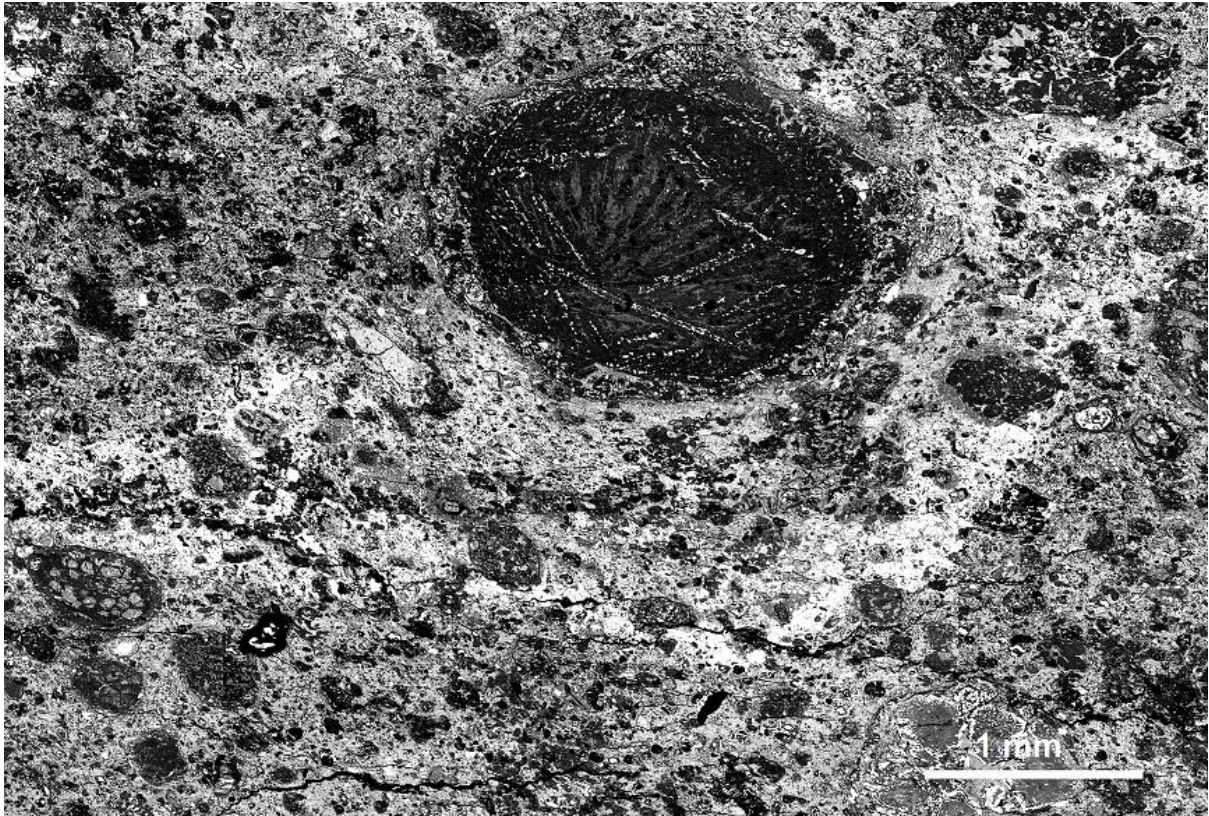
1165 Figure 4. High-angle annular dark-field imaging (HAADF) and X-Ray elemental maps of  
1166 Murchison matrix. For more details read the text.

1167

1168

1169

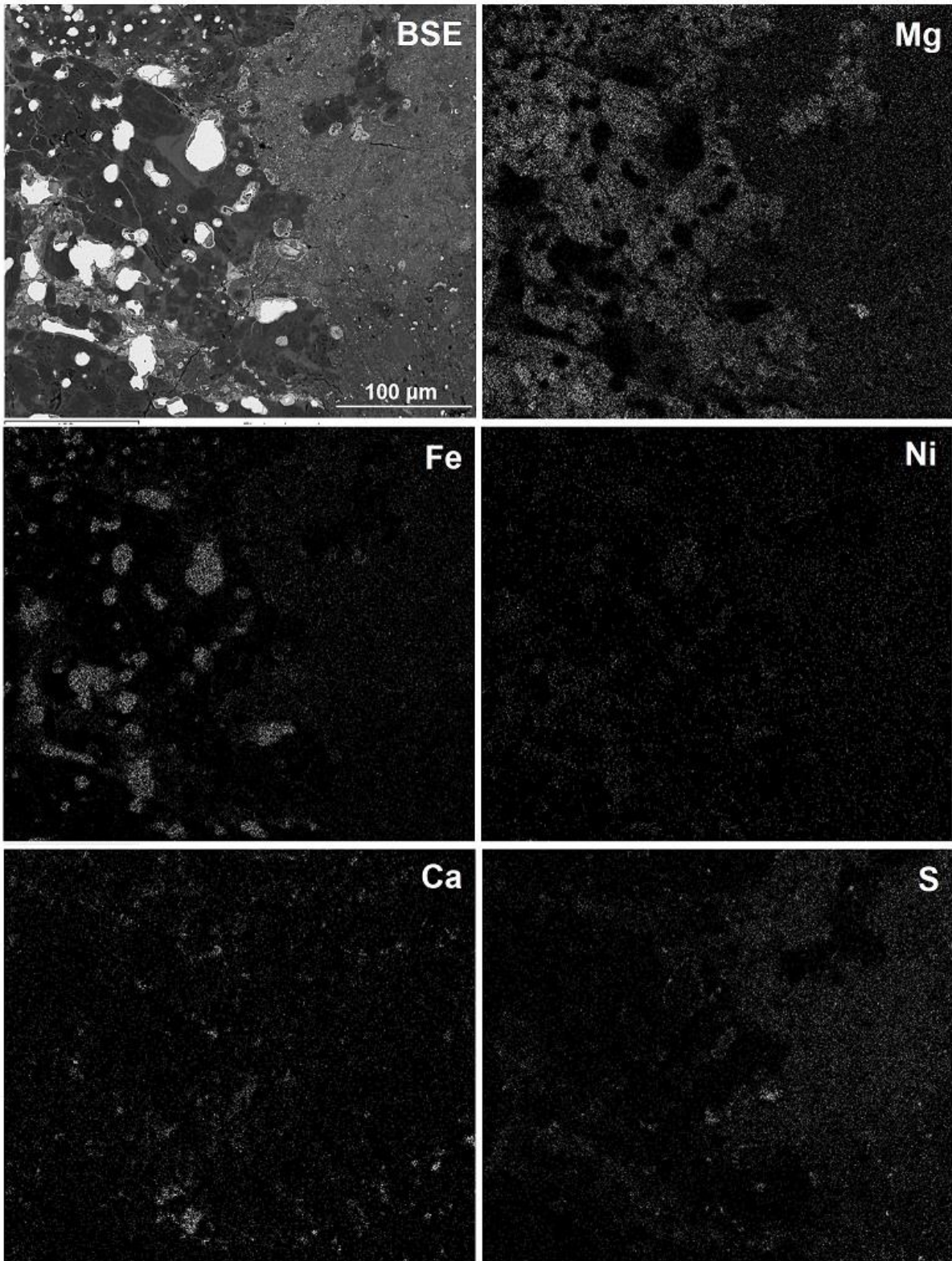




1170  
1171 Figure 5. BSE image of a cm-sized lens found in the MET 01070 CM2.0 chondrite. The lens  
1172 contains substantial amounts of fine-grained Ni-bearing sulphide and clumps of pentlandite  
1173 grains (Trigo-Rodríguez & Rubin, 2006; Rubin et al., 2007).

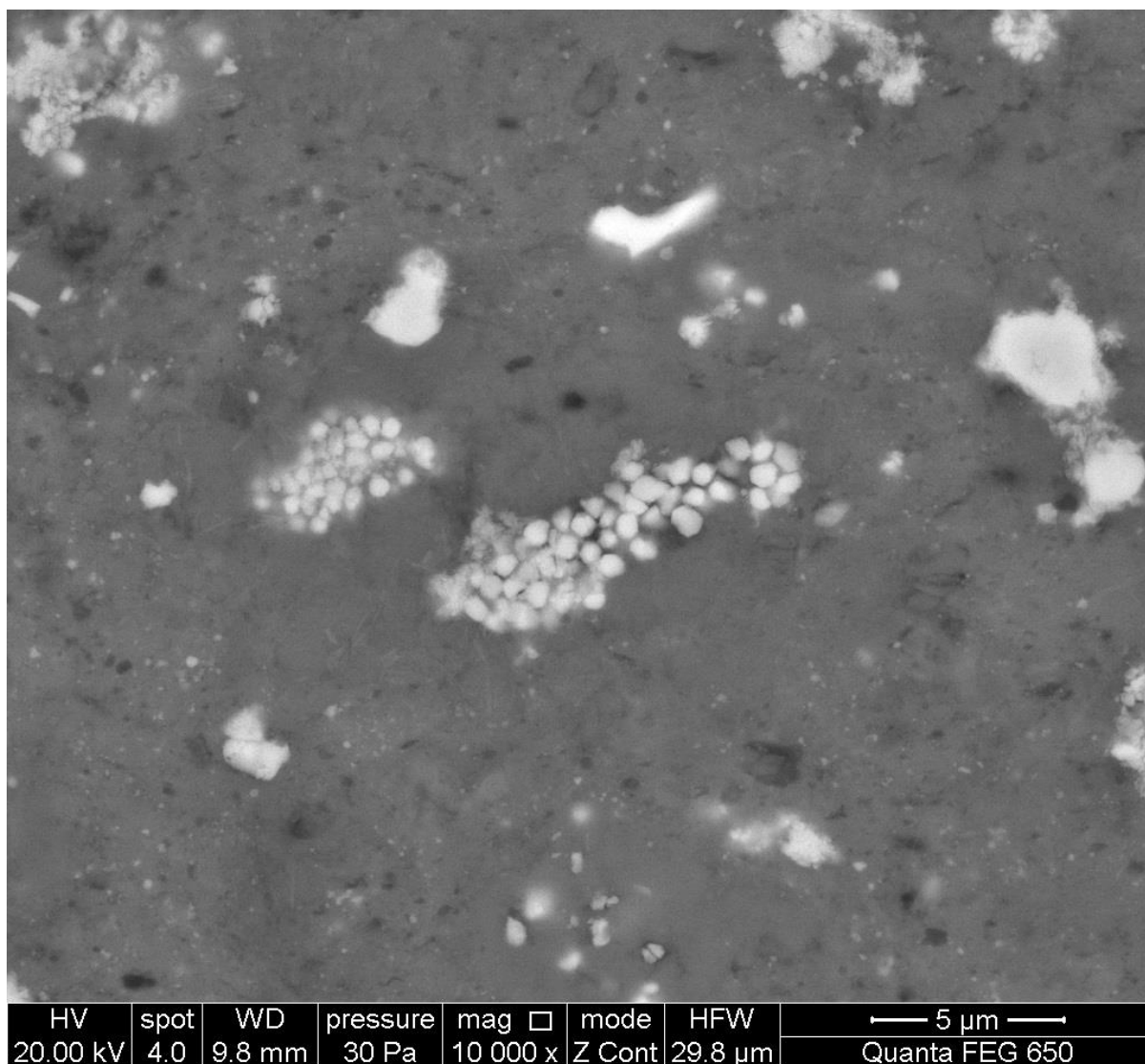
1174  
1175  
1176  
1177  
1178  
1179  
1180  
1181  
1182  
1183  
1184  
1185  
1186  
1187  
1188  
1189  
1190  
1191  
1192





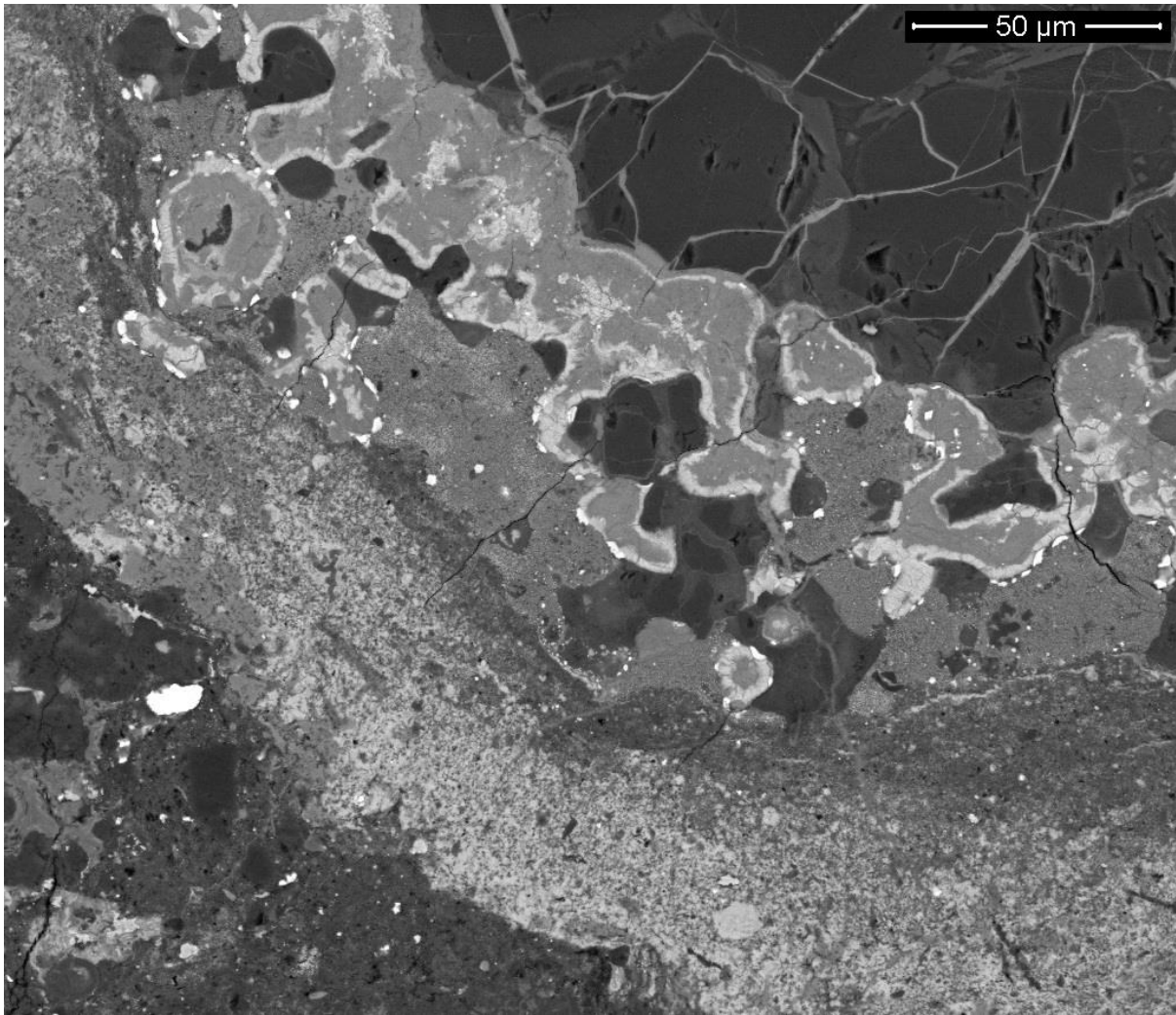
1193  
1194  
1195  
1196  
1197  
1198

Figure 6. BSE image and Mg, Fe, Ni, Ca and S X-ray maps of the CR2 chondrite Renazzo showing evidence of aqueous corrosion of metal grains and a chondrule border.



1200  
 1201  
 1202  
 1203  
 1204  
 1205  
 1206  
 1207  
 1208  
 1209  
 1210  
 1211  
 1212  
 1213  
 1214

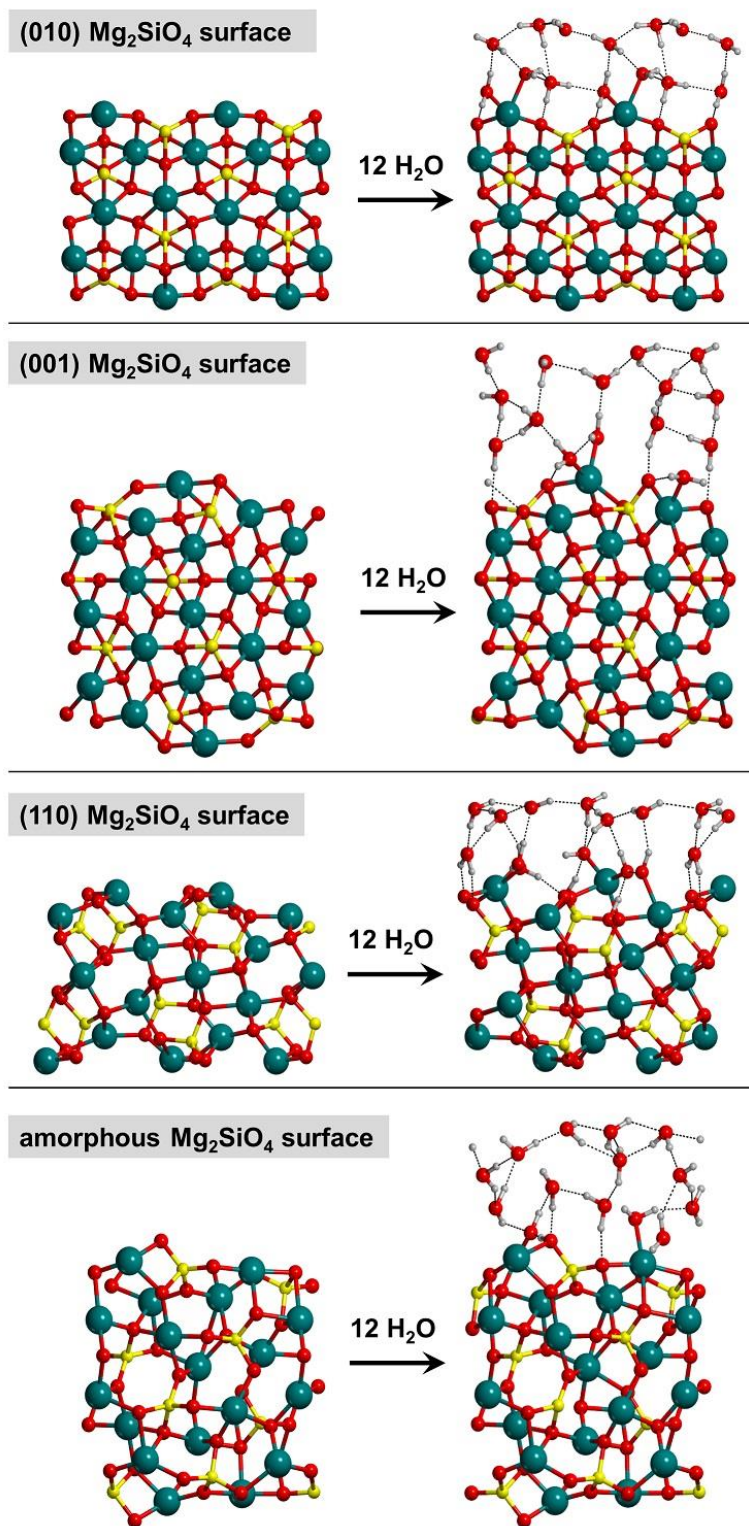
Figure 7. BSE image of the GRA 95229 CR chondrite showing pyrrhotite grains that were removed by the action of water, and the pores were filled by magnetite grains on the pore walls that belong to the meteorite matrix (for more details: Trigo-Rodríguez, 2015).



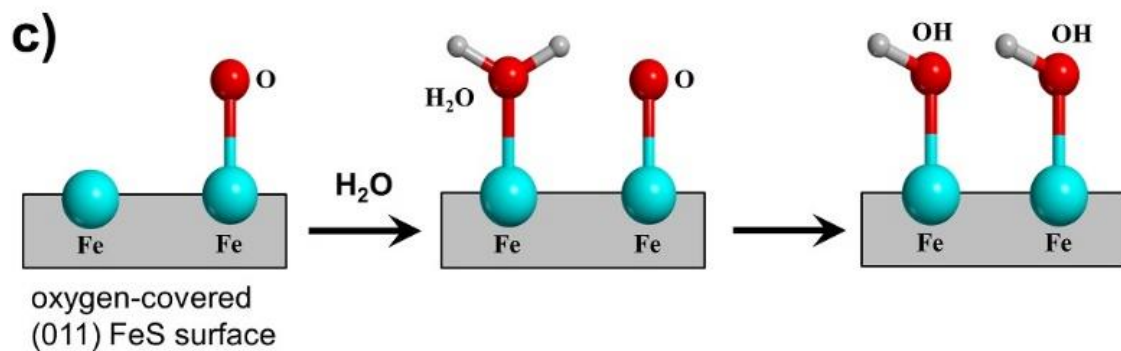
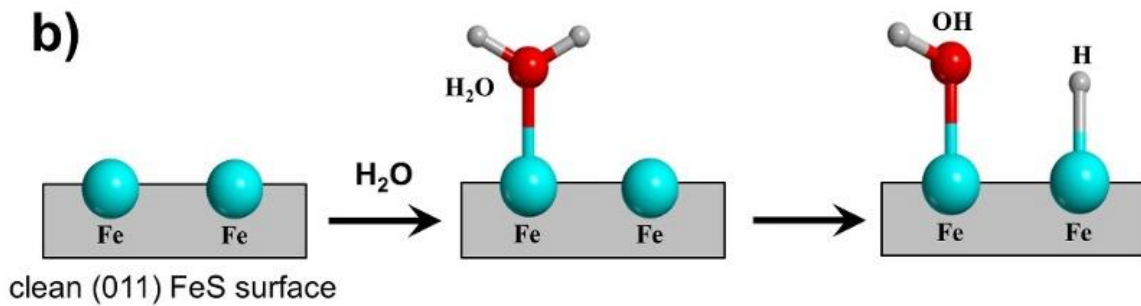
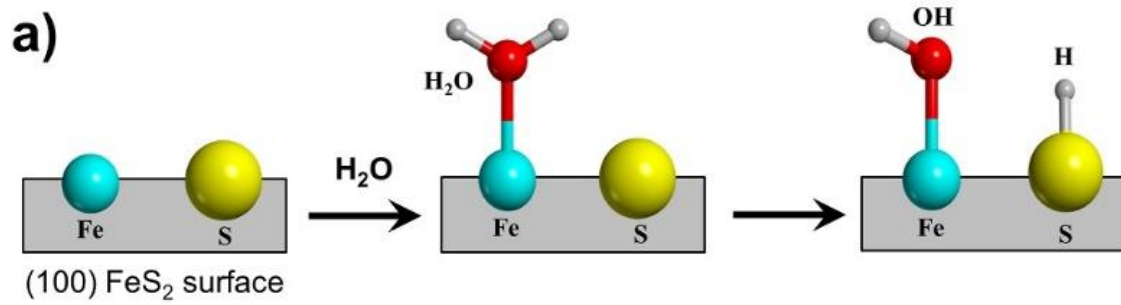
1215  
1216  
1217  
1218  
1219  
1220  
1221  
1222  
1223  
1224  
1225  
1226  
1227

**Figure 8.** BSE image of LAP 02342 showing the fine-grained texture of a S-rich rim surrounding a chondrule (located in the upper right). It is remarkable that the outer silicate border appears “eaten” as consequence of pervasive, but localized aqueous alteration. For more details (Moyano-Cambero et al., 2016; Nittler et al., 2019)





1228 Figure 9. Clean extended  $\text{Mg}_2\text{SiO}_4$  surfaces (left) and in interaction with 12 water  
 1229 molecules (right). For the (010) and (001) surfaces, the water molecules are molecularly  
 1230 adsorbed. For the (110) and amorphous surfaces, some water molecules interacting with the  
 1231 outermost  $\text{Mg}^{2+}$  cations are dissociated forming the  $\text{MgOH}$  and  $\text{SiOH}$  surface groups (Rimola  
 1232 & Trigo-Rodríguez, 2017).



1233  
1234  
1235  
1236  
1237  
1238  
1239

Figure 10. Schematic representation of the dissociation of water when in interaction with the (100)  $\text{FeS}_2$  surface (a) (Stirling et al., 2003), and the clean (b) and the oxygen-covered (c) (001) surface of FeS Mackinawite (Dzade et al., 2016).